ARTICLE

doi:10.1038/nature10362

The mechanism of membrane-associated steps in tail-anchored protein insertion

Malaiyalam Mariappan[1]*, Agnieszka Mateja[2]*, Malgorzata Dobosz[2], Elia Bove[2], Ramanujan S. Hegde[1]† & Robert J. Keenan[2]

Tail-anchored (TA) membrane proteins destined for the endoplasmic reticulum are chaperoned by cytosolic targeting factors that deliver them to a membrane receptor for insertion. Although a basic framework for TA protein recognition is now emerging, the decisive targeting and membrane insertion steps are not understood. Here we reconstitute the TA protein insertion cycle with purified components, present crystal structures of key complexes between these components and perform mutational analyses based on the structures. We show that a committed targeting complex, formed by a TA protein bound to the chaperone ATPase Get3, is initially recruited to the membrane through an interaction with Get2. Once the targeting complex has been recruited, Get1 interacts with Get3 to drive TA protein release in an ATPase-dependent reaction. After releasing its TA protein cargo, the now-vacant Get3 recycles back to the cytosol concomitant with ATP binding. This work provides a detailed structural and mechanistic framework for the minimal TA protein insertion cycle.

Approximately 5% of eukaryotic membrane proteins are anchored to the lipid bilayer by a single carboxy-terminal transmembrane domain[1–4] (TMD). These 'tail-anchored' proteins are found in virtually all cellular membranes and perform essential functions in processes including protein trafficking, degradation, cell death and membrane biogenesis. TA proteins in compartments of the secretory and endocytic pathways are first targeted to and inserted into the ER membrane by a post-translational targeting pathway conserved across eukaryotes[5–9] and archaea[10,11].

This pathway begins with a 'pre-targeting' factor that captures newly synthesized TA proteins through their TMDs near the ribosome[12,13]. In yeast, the pre-targeting factor is Sgt2, which assembles with Get3, Get4 and Get5 (also known as Mdy2) to form a TMD recognition complex[12,14,15]. Assembly of TMD recognition complexes permits substrates to be transferred from Sgt2 to Get3 in an ATP-dependent manner[12]. Get3 (TRC40, or ASNA1, in mammals) is a homodimeric ATPase whose conformation is regulated by its nucleotide state[16–20]. Both crystallographic and functional analyses support a model in which an ATP-bound, 'closed' dimer of Get3 binds substrates in a large hydrophobic groove that spans both subunits[16–18,20]. This substrate–Get3–nucleotide complex is therefore the committed targeting complex (Supplementary Discussion).

In yeast, genetic and physical interaction studies have identified the ER-localized membrane proteins Get1 and Get2 as potential receptors for Get3 (refs 7, 21). It is not known whether Get1, Get2 and Get3 constitute the minimal targeting and insertion machinery, how they function or what their essential roles are during TA protein insertion. In this Article, we combine functional reconstitution of TA protein insertion with structural analysis of key intermediate complexes to provide a mechanistic framework for the TA protein insertion cycle in *Saccharomyces cerevisiae*.

The minimal insertion machinery

We first reconstituted the TA protein insertion cycle with purified recombinant factors. A functional TA protein targeting complex was assembled and purified from *in vitro* translation reactions (Supplementary Fig. 1). The complex contained radio-labelled and epitope-tagged Sec61β (an ER-localized TA protein) bound to recombinant yeast Get3 in roughly the 2:1 ratio expected from structural studies. This recombinant targeting complex was functional as judged by membrane insertion of Sec61β into ER-derived yeast rough microsomes (yRMs) but not into protein-free liposomes (Fig. 1a). Microsomes from ΔGet1 and ΔGet2 yeast strains showed little insertion activity, whereas ΔGet3 microsomes were similar to wild-type yRMs. Sec61β insertion efficiency with the purified targeting complex was approximately two-fold higher than for Sec61β in crude translation reactions (data not shown), consistent with the observation that the latter contains a heterogeneous mixture of Sec61β complexes with other factors[8,13,22]. Thus, purified Get3–Sec61β is a committed targeting complex for Get1- and Get2-dependent membrane insertion.

The TA insertion defect of ΔGet1 and ΔGet2 microsomes is due solely to loss of Get1 and/or Get2. To show this, purified recombinant Get1 and Get2 (rGet1 and rGet2; Supplementary Fig. 2) produced from *Escherichia coli* were added to detergent extracts prepared from ΔGet1 or ΔGet2 yRMs, reconstituted into proteoliposomes and tested for function (Supplementary Fig. 3). Proteoliposomes from ΔGet1 yRMs were inactive for TA protein insertion, but were restored by replenishment with physiologic levels of rGet1 but not rGet2. ΔGet2 proteoliposomes required both rGet1 and rGet2 to restore insertion to near wild-type levels (Supplementary Fig. 3), as expected because Get1 is absent from ΔGet2 yRMs (Fig. 1a). We also biochemically depleted Get1 and Get2 from wild-type yRM and showed that the resulting insertion defect could be corrected by replenishment with rGet1 and rGet2 but with neither individually (Supplementary Fig. 4). Thus, rGet1 and rGet2 are fully functional in replacing their native counterparts during Get3-dependent TA protein insertion.

The lack of membrane proteins co-purifying with Get1 and Get2 (Supplementary Fig. 5), and the absence of other membrane proteins found in genetic studies[15,23,24], suggested that Get1 and Get2 are

[1]Cell Biology and Metabolism Program, National Institute of Child Health and Human Development, National Institutes of Health, Room 101, Building 18T, 18 Library Drive, Bethesda, Maryland 20892, USA. [2]Department of Biochemistry & Molecular Biology, The University of Chicago, Gordon Center for Integrative Science, Room W238, 929 East 57th Street, Chicago, Illinois 60637, USA. †Present address: MRC Laboratory of Molecular Biology, Hills Road, Cambridge CB2 0QH, UK.
*These authors contributed equally to this work.

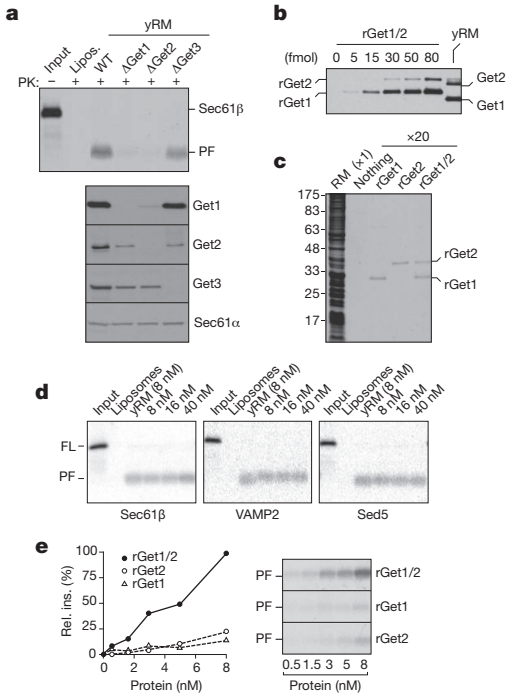

Figure 1 | Reconstitution of TA protein insertion with purified components. **a**, Yeast rough microsomes (yRMs) from the indicated strains were tested for insertion of purified Get3–Sec61β targeting complex (top) or by immunoblotting (bottom). The protease-protected fragment (PF) is diagnostic of successful insertion. Liposomes are a negative control. PK, proteinase K; WT, wild type. **b**, Quantification of Get1 and Get2 concentrations in yRMs by immunoblotting. **c**, Protein composition of yRMs and proteoliposomes containing recombinant proteins. Proteoliposomes in 20-fold relative excess were analysed. **d**, Insertion of purified targeting complexes into liposomes, yRMs, or rGet1/2 proteoliposomes. VAMP2 and Sed5, TMDs from rat VAMP2 or yeast Sed5. Concentrations of the Get1/2 complex are indicated FL, full length. **e**, Relative efficiency of insertion of purified Get3–Sec61β targeting complex into rGet1, rGet2 or rGet1/2 proteoliposomes. Autoradiographs and quantified data are shown.

sufficient for Get3-mediated TA protein insertion. Indeed, proteoliposomes containing physiologic concentrations of only rGet1 and rGet2 (Fig. 1b, c) were indistinguishable from yRM in mediating insertion of three different purified TA protein targeting complexes (Fig. 1d). Incorporating super-physiologic levels of rGet1 and rGet2 did not further improve insertion (Fig. 1d), and lower levels reduced overall insertion efficiency (Fig. 1e).

The recombinant system required both rGet1 and rGet2 (Fig. 1e), precisely mirroring the results *in vivo*[7] and in crude proteoliposomes (Supplementary Figs 3 and 4). Interaction analysis confirmed that rGet1 and rGet2 form a complex through their membrane domains in detergent solution (Supplementary Fig. 6), suggesting that during reconstitution they are incorporated as a complex. Taken together, the dependence on rGet1 and rGet2, their interaction with each other, their functionality in replacing the endogenous proteins and the high-efficiency insertion at native concentrations argue strongly that we have reconstituted physiologically relevant TA protein insertion with a defined targeting complex and only two membrane proteins.

The Get2c–Get3–ADP•AlF_4^- complex

Membrane targeting presumably involves an interaction between Get3 and the conserved cytosolic domains of Get1 and/or Get2 (Figs 2a and 3a and Supplementary Fig. 10). These fragments ('Get1c' and 'Get2c') did not interact with each other (Supplementary Figs 6 and 7), but both bound tightly to Get3 (Supplementary Figs 7 and 8) and inhibited the insertion of Sec61β into yRMs (Supplementary Fig. 8). The ability of Get3 to interact with either subunit of the Get1/2 complex suggested that each interaction might serve a different purpose in the insertion cycle.

The closed-dimer form of ADP•AlF_4^--bound Get3 probably mimics the TA substrate-bound conformation that targets to the membrane[16–18,20]. This Get3–ADP•AlF_4^- complex crystallized with Get2c, and we determined the structure to a resolution of 2.1 Å (Supplementary Table 1 and Supplementary Fig. 9). The structure reveals Get3 in a 'closed'-dimer conformation with ADP•AlF_4^- bound at each active site (Fig. 2b). Two Get2 fragments, each comprising two helices connected by a short linker, bind to equivalent sites on opposite faces of the symmetric Get3 homodimer. Each interface buries ~960 $Å^2$ of surface area, largely restricted to a single Get3 monomer (Fig. 2c, green, and

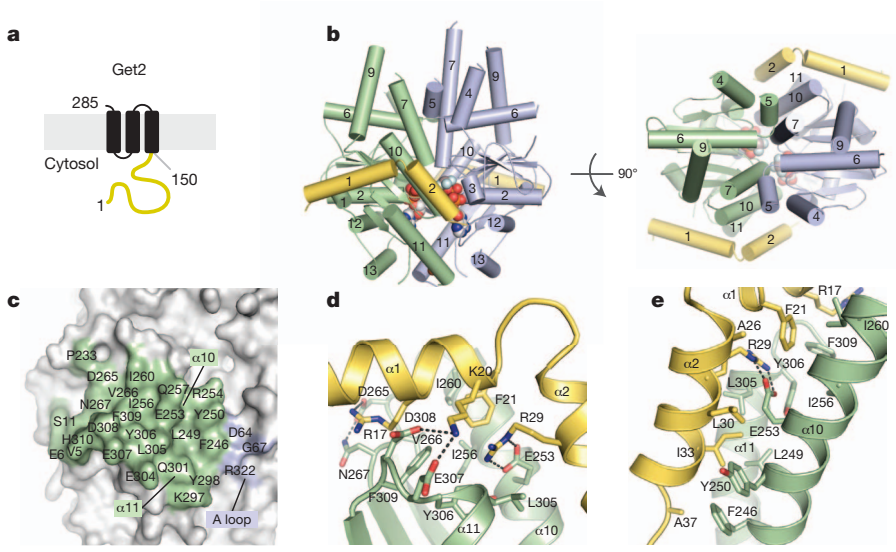

Figure 2 | Get2 fragment complex with ADP•AlF_4^--bound Get3. **a**, Predicted topology of *S. cerevisiae* Get2 with its large cytosolic-facing region (yellow). **b**, Structure of two Get2 fragments (yellow) bound to the closed Get3 dimer (green, blue). Two Mg^{2+}-ADP•AlF_4^- complexes and a zinc atom are indicated (spheres). An orthogonal view into the substrate-binding composite hydrophobic groove is shown on the right. **c**, Get3 residues in the Get2 interface are indicated. Most contacts are to one Get3 monomer (green); poorly ordered contacts are to the conserved A-loop ATPase motif. **d**, Close-up of interactions along helix α1 of Get2, including Arg 17, Lys 20 and Phe 21. **e**, Close-up of interactions along helix α2 of Get2, including the conserved salt bridge between Arg 29 and Glu 253.

Supplementary Fig. 10). Get3 residues within the interface undergo little conformational change on binding to Get2c (Supplementary Fig. 11). The amino-terminal helix of Get2 lies in a cleft defined at one end by short loops following helices α10 and α11 of Get3, and at the other end by the loop following helix α9 and the extreme N terminus of Get3 (Fig. 2d). Three conserved, negatively charged residues in Get3, namely Asp 265, Glu 307 and Asp 308, make direct contact with Get2c. The second helix of Get2 lies in a cleft defined by Get3 helices α10 and α11 (Fig. 2e). This surface is largely hydrophobic except for a conserved salt bridge between Glu 253 (Get3) and Arg 29 (Get2c). The C-terminal end of the Get2 fragment, which is not conserved, makes poorly ordered contacts with the adjacent Get3 monomer (Fig. 2c, blue).

The TA substrate-binding site in Get3 comprises a large hydrophobic groove spanning the α-helical subdomains of both monomers[16]. In the Get2c–Get3 complex, this groove is intact (Fig. 2b and Supplementary Fig. 20), suggesting that Get2 captures the closed Get3 targeting complex without disrupting the TA binding site. The long, flexible linker that tethers the helical N terminus of Get2 to its first TMD would facilitate this process. Thus, we propose that the Get2c–Get3–ADP•AlF_4^- structure represents a snapshot of the initial encounter between the closed-dimer targeting complex and the receptor.

The Get1c–Get3 complex

Get3 was also crystallized in the presence of Get1c. Whether or not ADP•AlF_4^- was present during crystallization, the Get3–Get1c crystals lacked nucleotide. We determined the structure of this nucleotide-free complex to a resolution of 3.0 Å (Supplementary Table 1 and Supplementary Fig. 9) and revealed Get3 in an 'open' conformation, with two Get1 fragments bound to equivalent sites on opposite faces of the symmetric Get3 homodimer (Fig. 3b). Each Get1 fragment adopts an antiparallel coiled-coil structure and buries ~1,030 $Å^2$ of surface area in a bipartite interface split evenly between the two Get3 subunits (Fig. 3c and Supplementary Fig. 10). As observed in the Get2c complex, Get3 residues on the interface undergo little conformational change on binding to Get1c (Supplementary Fig. 11). Binding to one Get3 monomer is primarily mediated by hydrophobic contacts between helix α2 of Get1c and the cleft defined by helices α10 and α11 of Get3 (Fig. 3c, d, green). Binding to the other monomer is mediated by helix α1 of Get1c, which interacts with Get3 helices α4 and α5, and by a six-residue loop in Get1c that directly contacts the ATP-binding site (Fig. 3c, e, blue; see below).

Importantly, many of the Get3 residues that contact Get1c also mediate interactions with Get2c (Supplementary Figs 10 and 11). For example, the conserved Arg 73 (Get1c)/Glu 253 (Get3) salt bridge almost perfectly mimics the Arg 29 (Get2c)/Glu 253 (Get3) interaction (Figs 2e and 3d). The presence of overlapping binding sites suggests that Get1 and Get2 cannot simultaneously occupy the same site on Get3, as illustrated by dissociation of the Get3–Get2c complex by Get1c (Supplementary Fig. 11). Previous work underscores the functional significance of this region of Get3: alanine substitutions within the shared interface, including F246A, Y250A, E253A and Y298A, have a strong loss-of-function phenotype in yeast[18]. Moreover, two of these positions, Tyr 250 and Glu 253, have been implicated in the ATP-dependent binding of Get4[25]. Thus, the α10–α11 region of Get3 is a binding hotspot that probably plays an important regulatory role at different stages of the targeting cycle.

The most striking aspect of the Get3–Get1c structure is how the Get1 coiled coil wedges between the Get3 subunits, completely disrupting the hydrophobic TA substrate-binding site (Fig. 3b). Such an interaction could effect substrate release from the Get3 targeting complex. However, parts of the bipartite Get1-binding site on Get3—including the ATPase motifs and portions of helices α4 and α5 (Fig. 3c, blue)—are buried in the ATP-bound, fully closed-dimer conformation. By contrast, the bipartite Get1-binding site is largely exposed to solvent in the Mg^{2+}-ADP-bound state[17,20] (Supplementary Fig. 12). This implies that ATP hydrolysis by the targeting complex is needed to expose the Get1-binding site on Get3 (Fig. 3c and Supplementary Fig. 12, green and blue). Once exposed, Get1 would complete the Get3 transition from closed to open, disrupting the hydrophobic groove to promote release of the TA substrate and ADP (which binds weakly to substrate-free Get3; Supplementary Fig. 18). Importantly, the rigid Get1 coiled coil is perpendicular to

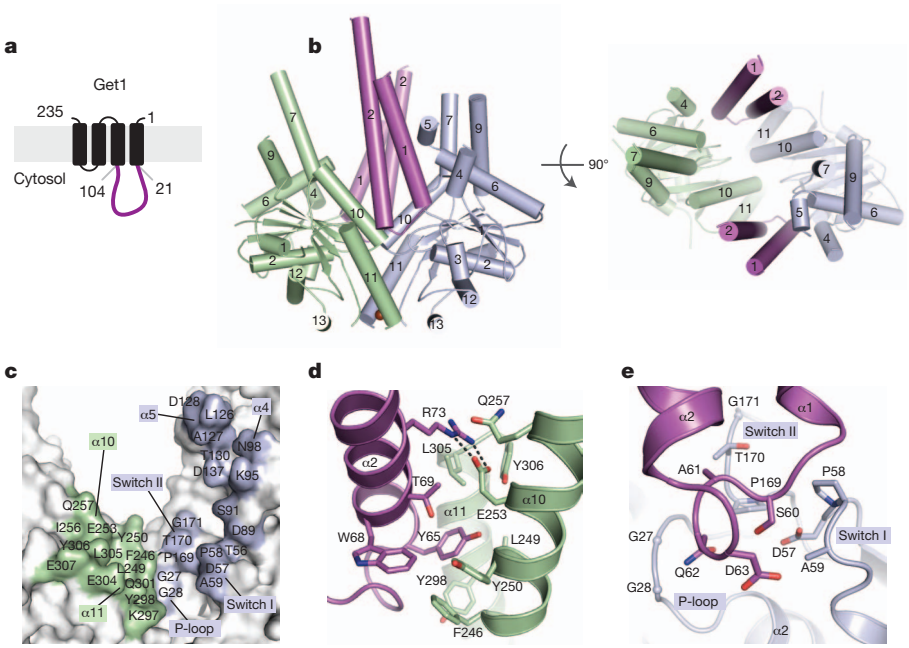

Figure 3 | Get1 fragment complex with Get3. **a**, Predicted topology of *S. cerevisiae* Get1 with a large cytosolic-facing region (magenta). **b**, Structure of two Get1 fragments (magenta) bound to the open dimer state of Get3 (green, blue). The composite hydrophobic groove is completely disrupted. **c**, Get3 residues in the Get1 interface are indicated; significant contacts are made to both monomers (green, blue), including the P-loop, switch I and switch II ATPase motifs. **d**, Close-up of interactions between Get1 helix α2 (magenta) and one Get3 monomer (green), including the conserved salt bridge between Arg 73 and Glu 253. This interface overlaps extensively with the Get2c binding surface (Fig. 2e and Supplementary Fig. 11). **e**, Close-up of interactions between the Get1 hairpin loop and the active site of the adjacent Get3 monomer (blue).

the plane of the membrane, thereby positioning the hydrophobic groove of Get3 parallel to the membrane. This implies that the TMD of a TA protein is precisely released along the membrane surface, presumably facilitating its subsequent insertion.

Targeting and substrate release

Conserved contacts between Get3–Get2 and Get3–Get1 were disrupted with point mutations (R17E and R73E, respectively), verified to prevent binding (Supplementary Fig. 13) and shown to reduce insertion in the reconstituted system sharply (Fig. 4a). When the substrate–Get3 interaction was monitored by crosslinking (Supplementary Fig. 14), Get1c, but not Get2c, was found to release TA substrate from Get3 (>50% at 500 nM; Fig. 4b). This activity was abolished by the R73E mutation that disrupts Get3–Get1c interactions (Fig. 4c). Thus, Get1c and Get2c both inhibit insertion (Supplementary Fig. 8), but for different reasons: Get1c causes premature substrate release whereas Get2c competitively precludes targeting.

When reconstituted into proteoliposomes at more-physiologic concentrations, neither rGet1 nor rGet2 was able to effect substrate release, whereas the complete rGet1/2 complex was active (Fig. 4d). Importantly, disrupting the Get3–Get1 interaction (with R73E) or the Get3–Get2 interaction (with R17E) abolished the ability of the rGet1/2 complex to stimulate substrate release (Fig. 4e). Thus, whereas Get1c at super-physiologic concentrations can drive substrate release on its own, full-length Get1 in the membrane is unable to do so at physiologic levels. In this context, Get1 requires Get2 (specifically its ability to bind Get3) to release substrate from Get3.

On the basis of the Get3–Get1c structure, ATP hydrolysis by the Get3 targeting complex is likely to be necessary for its interaction with Get1. Indeed, targeting complexes containing an ATPase-deficient Get3 mutant (D57N) were poorly inserted into proteoliposomes containing the rGet1/2 complex (Fig. 4f) despite no impairment of the interaction of Get3 (D57N) with substrate or the rGet1/2 complex (Supplementary Fig. 15 and data not shown). Analysis of the interaction between TA substrate and Get3 (D57N) revealed that the rGet1/2 complex was unable to induce release (Fig. 4d, e). Taken together, the results of the functional analysis indicate that the Get3–Get2 interaction is important for targeting, and that this step is a prerequisite for substrate release. Substrate release, in turn, depends on both ATP hydrolysis by Get3 and the ability of Get3 to interact with Get1.

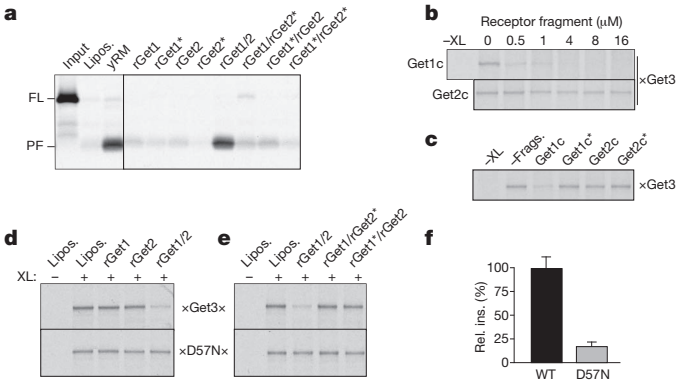

Figure 4 | Mutational analysis of the function of Get1, Get2 and Get3. **a**, Insertion assay with purified Get3–Sec61β targeting complex and proteoliposomes containing the indicated purified proteins. Liposomes and yRM are controls. Get1* and Get2* indicate mutants inactive in Get3 interaction (R73E and R17E, respectively). **b**, Substrate release from targeting complexes incubated with Get1c or Get2c; release was monitored by loss of the crosslink (XL) between radio-labelled substrate and Get3. Square brackets indicate concentration. **c**, As in **b**, with wild-type and mutant fragments at a concentration of 0.5 μM. **d**, Substrate interaction with Get3 or the ATPase-deficient Get3 (D57N) was assessed by crosslinking after incubation with liposomes or proteoliposomes containing the indicated recombinant proteins. **e**, As in **d**, but comparing wild-type and mutant complexes of Get1 and Get2. **f**, Relative efficiency of insertion (mean ± s.e.m.; $n = 6$) into rGet1/2 proteoliposomes with targeting complexes prepared from wild-type Get3 or Get3 (D57N).

ATP-dependent recycling

The ATP that Get3 hydrolyses before substrate release is apparently acquired from the *in vitro* translation reaction (and maintained during purification) because insertion proceeds efficiently without additional ATP in the purified system (Fig. 5a). This is consistent with structural analysis suggesting that nucleotide is shielded from bulk solvent in the fully closed Get3–ATP–substrate ternary complex (Supplementary Discussion). However, we (Supplementary Fig. 16) and others[6,17] have found that insertion reactions into crude yRMs, but not rGet1/2 proteoliposomes, are stimulated by ATP, non-hydrolysable ATP analogues or ADP. The explanation for this discrepancy proved to be the near-stoichiometric presence of Get3 on the Get1/2 complex in yRMs (Supplementary Fig. 5), but not on rGet1/2 proteoliposomes. Accordingly, binding Get3 to rGet1/2 proteoliposomes restored ATP dependence (Fig. 5b), whereas removing Get3 from yRM (by using ΔGet3 yeast) eliminated the ATP requirement for maximal insertion (Fig. 5c).

These results indicate that after TA substrate release, Get3 remains bound to microsomal membranes. In the nucleotide-free Get3–Get1c structure, which mimics this 'post-insertion' complex, residues within the conserved loop of Get1 (^{59}ISAQDN^{64}) insert into the Get3 active site (Fig. 3e) and deform it relative to the ADP•AlF_4^--bound conformation (Fig. 5d). Modelling ATP into the active site reveals steric and electrostatic clashes between Get1 and ATP, suggesting that free ATP should displace Get3 from Get1. Indeed, the Get3–Get1c interaction was quantitatively disrupted by micromolar concentrations of ATP (Fig. 5e). ADP was far less effective, and AMP failed to disrupt the Get3–Get1c complex. This ATP-dependent Get3 dissociation was also verified with full-length Get1 using pull-down assays (Supplementary Fig. 19). By contrast, none of the tested nucleotides

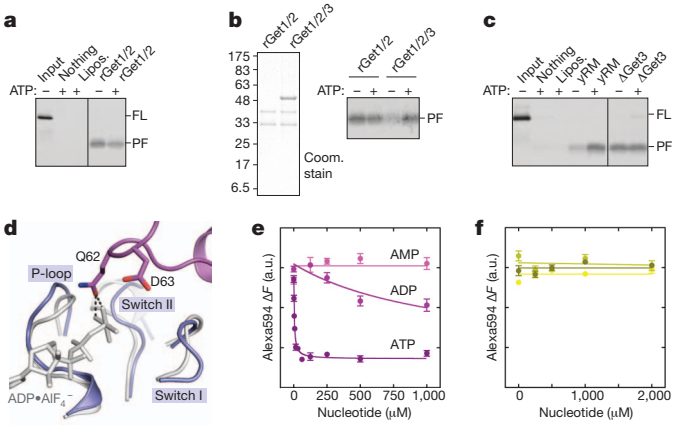

Figure 5 | ATP-dependent recycling of empty Get3 from Get1. **a**, Insertion activity of purified Get3–Sec61β targeting complex using the indicated vesicles with or without an ATP regenerating system. **b**, Proteoliposomes containing the rGet1/2 complex, or the rGet1/2 complex bound to Get3 (left panel), were tested for insertion activity of purified targeting complex in the presence or absence of ATP (right panel). Coom., Coomassie blue. **c**, Purified targeting complex was tested for insertion into wild-type yRMs or those from a ΔGet3 strain, with or without ATP. **d**, Close-up of the Get1c–Get3 complex (magenta and blue) modelled onto the active site of the closed, ADP•AlF_4^--bound Get3 dimer (grey). Steric (dashed lines) and electrostatic clashes between conserved residues in Get1 and the nucleotide γ-phosphate are apparent. **e**, Dissociation of Get3–Get1c, monitored by the change in fluorescence resonance energy transfer (ΔF), on titration with the indicated nucleotides. Curve fits of triplicate measurements (mean ± s.e.m.) are shown. a.u., arbitrary units. The reaction contained 10 nM Get3 (D57N) and 100 nM Get1c. **f**, As in **e**, but with 10 nM Get3 (D57N) and 200 nM Get2c.

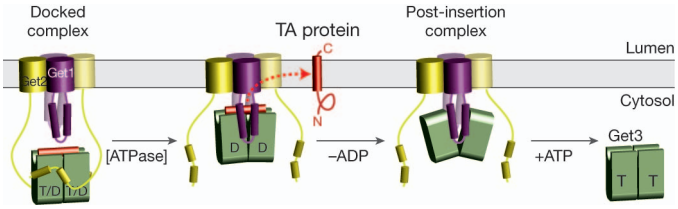

Figure 6 | Model for TA protein insertion. Nucleotide- and tail-anchored substrate-bound Get3 in a closed-dimer conformation forms the 'docked complex' by association with Get2. D, ADP; T, ATP. Following ATP hydrolysis, Get1 interacts with and orients Get3 along the membrane surface. This stabilizes the open-dimer conformation of Get3, disrupts the composite hydrophobic groove and promotes TA substrate release for membrane insertion. The Get3–Get1 post-insertion complex is dissociated by ATP binding, recycling Get3 back to the cytosol. See Supplementary Discussion for more details.

disrupted Get2c binding to Get3 (Fig. 5f). Thus, free ATP binding dissociates the Get1–Get3 complex to recycle Get3 from the membrane after TA substrate release.

A model for the insertion cycle

Figure 6 illustrates our working framework for the insertion cycle. Substrate-bound Get3 in the closed conformation and loaded with nucleotide (either ATP or ADP; see Supplementary Discussion) is captured at the membrane by the cytosolic domain of Get2. The apparently long and flexible Get2 tether may facilitate this initial encounter and bring the intact targeting complex near to the site of insertion. After this targeting step, Get1 mediates the post-targeting reactions of substrate release and insertion. Get1 binding to the targeting complex would be facilitated by partial destabilization of the closed dimer after ATP hydrolysis, and by the high local concentration of Get3 achieved by its recruitment through Get2. Binding to the rigid Get1 coiled coil would orient Get3 such that the substrate is in close proximity to the membrane. Moreover, by stabilizing the open conformation, Get1 binding would disrupt the Get3 hydrophobic groove and promote release of substrate and ADP. At present, we do not know whether the Get1/2 complex functions as a heterodimer or heterotetramer, although we favour the latter given the symmetric structure of the Get3 dimer. The released substrate would insert unassisted into the lipid bilayer directly[26,27] or would be chaperoned by the TMDs of the Get1/2 complex. Finally, the empty Get3 would be released from Get1 concomitant with ATP binding, and would be primed to accept the next substrate from the cytosolic pre-targeting complex for another round of targeting.

METHODS SUMMARY

Reagents and assays. Constructs, proteins and antibodies derived from earlier studies[8,13,16] are described in Methods. Antibodies against Get1 and Get2 were produced in rabbits. *In vitro* translation, insertion, crosslinking and immunoprecipitation were as described previously[8,13,28]. Get1 and Get2 (full length and fragments) were expressed in *E. coli* and purified by Ni-NTA chromatography; fragments were further purified by size exclusion chromatography. ^{35}S-labelled targeting complexes were affinity-purified from *in vitro* translation reactions containing recombinant Get3.

Liposomes, microsomes and proteoliposomes. Liposomes containing a 4:1 ratio of egg phosphatidylcholine and dipalmotylphosphatidylethanolamine were prepared by extrusion[27,29]. Yeast rough microsomes were prepared as before[30–33]. Proteoliposome reconstitutions from solubilized yRMs or purified Get1 and/or Get2 were done by optimizing (Supplementary Fig. 17) earlier methods[30,33,34].

Interaction analysis. Binding assays were performed by gel filtration and multi-angle light scattering, pull-down assays or fluorescence resonance energy transfer. Substrate release was monitored by amine-reactive crosslinking[8].

Structure determination. Complexes of Get3 with Get1c or Get2c were co-expressed in *E. coli* and purified by Ni-NTA and size exclusion chromatography. Diffraction data were collected at Advanced Photon Source beamline 21-IDG, Argonne National Laboratory. Structures were determined by molecular replacement in PHASER[35]. Refinement and model building was done using PHENIX[36] and COOT[37].

Full Methods and any associated references are available in the online version of the paper at www.nature.com/nature.

Received 7 April; accepted 13 July 2011.
Published online 24 August 2011.

1. Kutay, U., Hartmann, E. & Rapoport, T. A. A class of membrane proteins with a C-terminal anchor. *Trends Cell Biol.* **3,** 72–75 (1993).
2. Beilharz, T., Egan, B., Silver, P. A., Hofmann, K. & Lithgow, T. Bipartite signals mediate subcellular targeting of tail-anchored membrane proteins in *Saccharomyces cerevisiae*. *J. Biol. Chem.* **278,** 8219–8223 (2003).
3. Kalbfleisch, T., Cambon, A. & Wattenberg, B. W. A bioinformatics approach to identifying tail-anchored proteins in the human genome. *Traffic* **8,** 1687–1694 (2007).
4. Kriechbaumer, V. *et al.* Subcellular distribution of tail-anchored proteins in *Arabidopsis*. *Traffic* **10,** 1753–1764 (2009).
5. Favaloro, V., Spasic, M., Schwappach, B. & Dobberstein, B. Distinct targeting pathways for the membrane insertion of tail-anchored (TA) proteins. *J. Cell Sci.* **121,** 1832–1840 (2008).
6. Favaloro, V., Vilardi, F., Schlecht, R., Mayer, M. P. & Dobberstein, B. Asna1/TRC40-mediated membrane insertion of tail-anchored proteins. *J. Cell Sci.* **123,** 1522–1530 (2010).
7. Schuldiner, M. *et al.* The GET complex mediates insertion of tail-anchored proteins into the ER membrane. *Cell* **134,** 634–645 (2008).
8. Stefanovic, S. & Hegde, R. S. Identification of a targeting factor for posttranslational membrane protein insertion into the ER. *Cell* **128,** 1147–1159 (2007).
9. Borgese, N. & Fasana, E. Targeting pathways of C-tail-anchored proteins. *Biochim. Biophys. Acta* **1808,** 937–946 (2011).
10. Sherrill, J., Mariappan, M., Dominik, P., Hegde, R. S. & Keenan, R. J. A conserved archaeal pathway for tail-anchored membrane protein insertion. *Traffic* doi:10.1111/j.1600-0854.2011.01229.x (3 July 2011).
11. Borgese, N. & Righi, M. Remote origins of tail-anchored proteins. *Traffic* **11,** 877–885 (2010).
12. Wang, F., Brown, E. C., Mak, G., Zhuang, J. & Denic, V. A chaperone cascade sorts proteins for posttranslational membrane insertion into the endoplasmic reticulum. *Mol. Cell* **40,** 159–171 (2010).
13. Mariappan, M. *et al.* A ribosome-associating factor chaperones tail-anchored membrane proteins. *Nature* **466,** 1120–1124 (2010).
14. Chang, Y.-W. *et al.* Crystal structure of Get4-Get5 complex and its interactions with Sgt2, Get3, and Ydj1. *J. Biol. Chem.* **285,** 9962–9970 (2010).
15. Jonikas, M. C. *et al.* Comprehensive characterization of genes required for protein folding in the endoplasmic reticulum. *Science* **323,** 1693–1697 (2009).
16. Mateja, A. *et al.* The structural basis of tail-anchored membrane protein recognition by Get3. *Nature* **461,** 361–366 (2009).
17. Bozkurt, G. *et al.* Structural insights into tail-anchored protein binding and membrane insertion by Get3. *Proc. Natl Acad. Sci. USA* **106,** 21131–21136 (2009).
18. Suloway, C. J., Chartron, J. W., Zaslaver, M. & Clemons, W. M. Jr. Model for eukaryotic tail-anchored protein binding based on the structure of Get3. *Proc. Natl Acad. Sci. USA* **106,** 14849–14854 (2009).
19. Yamagata, A. *et al.* Structural insight into the membrane insertion of tail-anchored proteins by Get3. *Genes Cells* **15,** 29–41 (2010).
20. Hu, J., Li, J., Qian, X., Denic, V. & Sha, B. The crystal structures of yeast Get3 suggest a mechanism for tail-anchored protein membrane insertion. *PLoS ONE* **4,** e8061 (2009).
21. Auld, K. L. *et al.* The conserved ATPase Get3/Arr4 modulates the activity of membrane-associated proteins in *Saccharomyces cerevisiae*. *Genetics* **174,** 215–227 (2006).
22. Leznicki, P., Clancy, A., Schwappach, B. & High, S. Bat3 promotes the membrane integration of tail-anchored proteins. *J. Cell Sci.* **123,** 2170–2178 (2010).
23. Schuldiner, M. *et al.* Exploration of the function and organization of the yeast early secretory pathway through an epistatic miniarray profile. *Cell* **123,** 507–519 (2005).
24. Costanzo, M. *et al.* The genetic landscape of a cell. *Science* **327,** 425–431 (2010).
25. Chartron, J. W., Suloway, C. J. M., Zaslaver, M., a. & Clemons, W. M. Structural characterization of the Get4/Get5 complex and its interaction with Get3. *Proc. Natl Acad. Sci. USA* **107,** 12127–12132 (2010).
26. Renthal, R. Helix insertion into bilayers and the evolution of membrane proteins. *Cell. Mol. Life Sci.* **67,** 1077–1088 (2010).
27. Brambillasca, S. *et al.* Transmembrane topogenesis of a tail-anchored protein is modulated by membrane lipid composition. *EMBO J.* **24,** 2533–2542 (2005).
28. Sharma, A., Mariappan, M., Appathurai, S. & Hegde, R. S. *In vitro* dissection of protein translocation into the mammalian endoplasmic reticulum. *Methods Mol. Biol.* **619,** 339–363 (2010).
29. Brambillasca, S., Yabal, M., Makarow, M. & Borgese, N. Unassisted translocation of large polypeptide domains across phospholipid bilayers. *J. Cell Biol.* **175,** 767–777 (2006).
30. Panzner, S., Dreier, L., Hartmann, E., Kostka, S. & Rapoport, T. A. Posttranslational protein transport in yeast reconstituted with a purified complex of Sec proteins and Kar2p. *Cell* **81,** 561–570 (1995).
31. Rothblatt, J. A. & Meyer, D. I. Secretion in yeast: reconstitution of the translocation and glycosylation of alpha-factor and invertase in a homologous cell-free system. *Cell* **44,** 619–628 (1986).
32. Hansen, W., Garcia, P. D. & Walter, P. *In vitro* protein translocation across the yeast endoplasmic reticulum: ATP-dependent posttranslational translocation of the prepro-alpha-factor. *Cell* **45,** 397–406 (1986).

33. Gorlich, D. & Rapoport, T. A. Protein translocation into proteoliposomes reconstituted from purified components of the endoplasmic reticulum membrane. *Cell* **75,** 615–630 (1993).
34. Fons, R. D., Bogert, B. A. & Hegde, R. S. Substrate-specific function of the translocon-associated protein complex during translocation across the ER membrane. *J. Cell Biol.* **160,** 529–539 (2003).
35. McCoy, A. J. *et al.* Phaser crystallographic software. *J. Appl. Crystallogr.* **40,** 658–674 (2007).
36. Adams, P. D. *et al.* PHENIX: a comprehensive Python-based system for macromolecular structure solution. *Acta Crystallogr. D* **66,** 213–221 (2010).
37. Emsley, P. & Cowtan, K. Coot: model-building tools for molecular graphics. *Acta Crystallogr. D* **60,** 2126–2132 (2004).

Supplementary Information is linked to the online version of the paper at www.nature.com/nature.

Acknowledgements Data were collected at beamline 21-IDG at the Advanced Photon Source (APS), Argonne National Laboratory, and we thank the beamline staff for support. We thank T. Dever for yeast strains, T. Rapoport for the Sec61α antibody, M. Downing for technical assistance, members of the Hegde, Keenan and E. Perozo labs and D. Freymann for advice, and A. Shiau and S. Shao for discussions and comments on the manuscript. Use of the APS, an Office of Science User Facility operated for the US Department of Energy (DOE) Office of Science by Argonne National Laboratory, was supported by the US DOE under contract no. DE-AC02-06CH11357. This work was supported by the Intramural Research Program of the NIH (to R.S.H.), the Camille and Henry Dreyfus Postdoctoral Program in Environmental Chemistry (to R.J.K. and E.B.), an Edward Mallinckrodt, Jr. Foundation Grant (to R.J.K.) and NIH Grant R01 GM086487 (to R.J.K.).

Author Contributions A.M., M.D. and E.B. produced, purified and characterized recombinant Get1, Get2 (full length and fragments) and Get3. M.M. and R.S.H. performed the reconstitution experiments, including the substrate release and membrane insertion assays. A.M., M.D. and R.J.K. carried out crystallization and structure determination as well as the interaction analyses. R.S.H. and R.J.K. designed the project. M.M., R.S.H. and R.J.K. wrote the paper. All authors discussed the results and commented on the manuscript.

Author Information Atomic coordinates and structure factors for *S. cerevisiae* Get3 in complex with Get1(21–104) and for Mg^{2+}-ADP•AlF_4^--bound *S. cerevisiae* Get3 in complex with Get2(1–38) have been deposited in the Protein Data Bank under accession codes 3ZS8 and 3ZS9, respectively. Reprints and permissions information is available at www.nature.com/reprints. The authors declare no competing financial interests. Readers are welcome to comment on the online version of this article at www.nature.com/nature. Correspondence and requests for materials should be addressed to R.J.K. (bkeenan@uchicago.edu) or R.S.H. (hegde.science@gmail.com).

METHODS

Reagents and basic procedures. Antibodies against Get1 (residues 61–74) and Get2 (residues 2–12) were generated against synthetic peptides conjugated to KLH via terminal cysteines. Antibody against yeast Get3 was against the whole recombinant protein. Antibody production was by LAMPIRE Biological Laboratories. The antibodies against the 3F4 tag and Sec61β have been described previously[8]. The Sec61α antibody was a gift from Tom Rapoport (Harvard University). DeoxyBigCHAP (DBC) was obtained from Calbiochem. Yeast strains were from Open Biosystems collections and were provided by Tom Dever. The following lipids were obtained from Avanti Polar Lipids: egg phosphatidylcholine (PC), 1-palmitoyl-2-oleoyl-*sn*-glycero-3-phosphoethanolamine (PE) and 1,2-dipalmitoyl-*sn*-glycero-3-phosphoethanolamine-*N*-lissamine rhodamine B (rhodamine-PE). Each lipid was dissolved and stored in chloroform at −20 °C or −80 °C. Protease inhibitor cocktail was from Roche (EDTA-free Complete tablets) and dissolved as a ×25 stock in aqueous buffer just before use. *In vitro* translation, chemical crosslinking and immunoprecipitations were as described previously[8,13,28].

Preparation of proteins for functional analysis. The genes encoding full-length or cytosolic fragments of *S. cerevisiae* Get1, Get2 and Get3 were amplified by PCR from genomic DNA. Site-directed mutants were obtained by QuikChange mutagenesis (Stratagene). Unless otherwise noted, all constructs were subcloned into a pET28 derivative (Novagen) modified to incorporate a tobacco etch virus (TEV) protease cleavage site between an N-terminal 6×His tag and the polylinker. All constructs were verified by DNA sequencing.

Expression and purification of full-length Get3 (wild type and D57N) was carried out as described previously[16]. Full-length Get1 and Get2 (wild type and mutants) were expressed in *E. coli* Rosetta2/pLysS (Novagen) using the Overnight Express Autoinduction System 1 (Novagen). Cells were disrupted in buffer A (50 mM HEPES, pH 8.0, 500 mM NaCl, 10 mM imidazole, 5% glycerol) with 1 mM PMSF using a high-pressure microfluidizer (Avestin), and the insoluble pellet was isolated by centrifugation. This pellet was washed in buffer A, recentrifuged and solubilized for 1 h at 4 °C in buffer A containing 0.5% *n*-dodecyl-*N*,*N*-dimethylamine-*N*-oxide (LDAO). The detergent-soluble fraction was then subjected to nickel-affinity chromatography (Ni-NTA agarose, Qiagen) in buffer A containing 30 mM imidazole and 0.1% LDAO. Protein was eluted at ~1 mg ml^{-1} in buffer A containing 200 mM imidazole and 0.1% LDAO, and stored in aliquots at −80 °C. Protein concentrations were determined using calculated A_{280} extinction coefficients.

The cytosolic Get1 fragment (residues 21–104) was expressed for 3 h at 37 °C (wild type) or overnight at 25 °C (R73E mutant) in *E. coli* BL21(DE3)/pRIL (Novagen), following induction with 0.1 mM IPTG. Cells were disrupted in buffer B (50 mM Tris, pH 7.5, 500 mM NaCl, 10 mM imidazole, 5% glycerol, 5 mM β-mercaptoethanol) with 1 mM PMSF using a microfluidizer. After clearing by centrifugation, the supernatant was batch-purified by nickel-affinity chromatography. Protein was eluted in buffer B containing 200 mM imidazole, dialyzed into 10 mM Tris, pH 7.5, 250 mM NaCl and 40% glycerol, and then stored at −80 °C. This was typically followed by gel filtration (Superdex 200 10/300 GL, GE Healthcare) in 10 mM Tris, pH 7.5, and 200 mM NaCl. Fractions were pooled and stored in aliquots at −80 °C. Protein concentrations were determined using calculated A_{280} extinction coefficients.

The cytosolic Get2 fragment (residues 1–38 or 1–106; wild type and R17E) was expressed with an N- or C-terminal 6×His tag overnight at 25 °C and purified by nickel-affinity chromatography as described above for the Get1 fragment. After dialysis against 10 mM Tris, pH 7.5, and 200 mM NaCl, proteins were further purified by gel filtration in 10 mM Tris, pH 7.5, and 150 mM NaCl. Fractions were pooled, concentrated and stored in aliquots at −80 °C. Protein concentration was determined by BCA (Pierce).

Preparation of liposomes. The standard liposome mixture typically contained PC:PE:rhodamine-PE at a mass ratio of 8:1.9:0.1. Rhodamine-PE serves as a tracer to follow the lipid recovery. Lipid solutions were mixed in the above ratios as chloroform stocks, adjusted to 10 mM DTT and dried in a glass tube by centrifugation under vacuum (SpeedVac, Eppendorf) for 12 h. Lipid films were hydrated to a final concentration of 20 mg ml^{-1} in lipid buffer (50 mM HEPES-KOH, pH 7.4, 15% glycerol) and mixed end to end for 6 h at 25 °C with intermittent vortexing. The milky and uniform suspension was subjected to three freeze–thaw cycles (freeze in liquid nitrogen; thaw at 37 °C) and extruded at 65 °C 11 times through 100-nm polycarbonate membranes using an Avanti mini-extruder[27,29]. Single-use aliquots (100 µl) of the final clear liposome solution were flash-frozen in liquid nitrogen and stored at −80 °C.

Purification of recombinant targeting complex. The DNA template for the double-Strep-tagged human Sec61β was generated by PCR using a 5′ oligonucleotide that encodes the T7 promoter, start codon and tag. This template was transcribed and translated in RRL as described previously[28], but with 0.15 mg ml^{-1} His-Get3 (added from a 20 mg ml^{-1} stock in 10 mM Tris-HCl, pH 7.5, 100 mM NaCl and 40% glycerol). A 2-ml translation reaction was diluted twofold with ice-cold column buffer (20 mM HEPES-KOH, pH 7.4, 100 mM potassium acetate, 2 mM magnesium acetate, 1 mM DTT) and centrifuged for 30 min at 540,960*g* in a TLA100.3 rotor at 4 °C. The post-ribosomal supernatant was bound to a 400-µl DEAE-Sepharose fast-flow column at 4 °C, washed with column buffer and eluted with a buffer containing 50 mM HEPES-KOH, pH 7.4, 320 mM potassium acetate, 7 mM magnesium acetate and 1 mM DTT. The elution was passed over 200 µl Strep-Tactin agarose (IBA, Germany) one to three times. After washing with four column volumes of Strep-Tactin buffer (50 mM HEPES-KOH, pH 7.4, 10% glycerol, 150 mM potassium acetate, 7 mM magnesium acetate, 1 mM DTT) at 4 °C, bound proteins were eluted with 5 × 50 µl Strep-Tactin buffer containing 10 mM Desthiobiotin (Novagen). The peak fractions, measured by counting radioactivity, were pooled. The final sample contained ~10,000 c.p.m. µl^{-1}. The concentration of Get3 in the final sample was estimated to be ~80 nM. Thus, the targeting complex in our typical preparation has a concentration of ~40 nM, assuming a 2:1 ratio of Get3 to Sec61β. This was either used immediately or frozen in aliquots in liquid nitrogen and stored at −80 °C. Targeting complexes containing the TMDs of rat VAMP2 and *S. cerevisiae* Sed5 in place of the Sec61β TMD were made similarly.

Insertion assay. Post-translational insertion assay was performed as described before[8], with the following minor modifications. For a standard reaction, 8 µl of purified targeting complex was mixed with 1 µl of ATP regenerating system (2 mM ATP, 10 mM creatine phosphate and 40 µg ml^{-1} creatine kinase) and 1 µl of yRMs, liposomes, reconstituted proteoliposomes or a matched buffer. ATP regenerating system was omitted in some reactions as indicated in the figure legends. After incubation at 32 °C for 30 min, the samples were treated with proteinase K (0.5 mg ml^{-1}) for 60 min on ice, and the protease digestion was terminated with 5 mM PMSF and transferred to 100 µl of boiling 1% SDS as described previously[8]. The protease-protected fragment was then immunoprecipitated using the 3F4 antibody directed against the C terminus of the Sec61β construct. Immunoprecipitated products were analysed by SDS–polyacrylamide gel electrophoresis (SDS–PAGE) and quantified by phosphor imaging.

Preparation of rough microsomes from yeast. Yeast microsomes were prepared by modifications of the methods previously described[30–32,38]. TAP-tagged Get1 (Open Biosystems) or Get deletion strains (gift from T. Dever) were grown at 30 °C to a density of 2A_{600} U in 1 l of YPD medium containing 2% glucose. Cells were collected by centrifugation at 3,000*g* for 5 min and washed twice with ice-cold distilled water. All subsequent steps were on ice or at 4 °C. The cell pellet was resuspended in 50 ml of homogenization buffer (20 mM HEPES-KOH, pH 7.4, 100 mM potassium acetate, 2 mM magnesium acetate) and centrifuged for 5 min at 3,000*g*. The resulting cell pellet was resuspended in homogenization buffer containing 2 mM DTT and protease inhibitor cocktail (Roche) at a concentration of 1 ml per gram of cell pellet. Pre-chilled glass beads were added (3 g ml^{-1} of suspension), and cell lysis was induced as follows: the tube was vigorously shaken up and down over a 50-cm path at ~1–2 cycles s^{-1} for three 1-min periods separated by 1 min chilling on ice. Approximately 50% of the cells were broken by this method as visualized by microscopy. The fluid phase was drained off through a fine nylon mesh into a JA17 tube and spun at 10,000*g* for 10 min. The post-mitochondrial supernatant was briefly centrifuged in a MLA80 rotor at 339,707*g* for 8 min. Each 2 ml of the clear supernatant was layered on 1 ml of 0.67 M sucrose cushion in homogenization buffer and centrifuged for 30 min in a TLA100.3 rotor at 265,070*g*. The resulting membrane pellet was resuspended in homogenization buffer containing 250 mM sucrose and 2 mM DTT to a final standard concentration of 100A_{280} (measured after solubilization in 1% SDS). At this concentration, 1 µl yRM is defined as two equivalents (equiv.). One litre of culture yielded about 2,400 equiv. Aliquots were frozen in liquid nitrogen and stored at −80 °C.

Depletion of Get1 and Get2 from microsomal extract. TAP-Get1 yRMs (1.5 ml, or 1,500 equiv.) were adjusted to 1% DBC in solubilization buffer (50 mM HEPES-KOH, pH 7.4, 500 mM potassium acetate, 5 mM magnesium acetate, 250 mM sucrose, 1 mM DTT and protease inhibitor cocktail). After 10 min incubation on ice, the detergent extract was centrifuged at 540,960*g* for 30 min in a TLA100.3 rotor at 4 °C. The supernatant (yRM extract) was incubated with 0.1 ml of IgG Sepharose (GE Healthcare) for 1 h at 25 °C. The unbound fraction was incubated with 0.1 ml of anti-Get2 antibodies coupled to protein-A agarose for 1 h at 25 °C. The flow-through was finally incubated with a mixture of 0.1 ml each of anti-Get1 and anti-Get2-antibodies coupled to protein-A agarose for 1 h at 25 °C. The flow-through from this column was used for reconstitution studies. It should be noted that a residual amount of the Get1/2 complex is sufficient to achieve the maximal insertion under *in vitro* conditions. Therefore, multiple rounds of depletion of the Get1/2 complex (with at least ~95% depletion) were necessary to fully deplete insertion activity. For purification of TAP-Get1 (and

associated proteins), the IgG Sepharose resin from above was washed with low-salt buffer (10 mM Tris, pH 7.4, 150 mM NaCl, 10% glycerol, 0.25% DBC and 1 mM DTT) and eluted with 70 U TEV-protease (Invitrogen) overnight at 4 °C. The TEV elution was adjusted to 2.5 mM $CaCl_2$, and incubated with calmodulin Sepharose (GE Healthcare) for 90 min at 4 °C. The beads were washed with low-salt buffer containing $CaCl_2$ and eluted with low-salt buffer containing 5 mM EGTA. The eluted proteins were precipitated with TCA and analysed by SDS–PAGE.

Reconstitution of proteoliposomes from microsome extracts. Following earlier methods[30,33,34], yRMs were adjusted to a concentration of 1 equiv. μl^{-1} in the following conditions: 50 mM HEPES-KOH, pH 7.4, 500 mM potassium acetate, 5 mM magnesium acetate, 250 mM sucrose, 1 mM DTT, 1% DBC and protease inhibitor cocktail. After 10 min on ice, the ribosomes were removed by centrifugation at 540,960*g*. for 30 min in a TLA100.3 rotor at 4 °C. Typically, 100 µl of this clarified yRM extract was mixed with 10 µl of liposomes (200 µg) and 50 mg of Biobeads SM2 (Bio-Rad). The Biobeads were prewashed extensively ahead of time with methanol and water. The mixture was incubated for 12–16 h with gentle overhead mixing at 4 °C. The fluid phase was separated from the beads, diluted with five volumes of ice-cold distilled water and sedimented in a TLA100.3 rotor in micro-test tubes at 304,290*g* for 30 min at 4 °C. The proteoliposomes were resuspended in 25 µl of membrane buffer (50 mM HEPES-KOH, pH 7.4, 100 mM potassium acetate, 5 mM magnesium acetate, 250 mM sucrose, and 1 mM DTT).

Reconstitution of proteoliposomes with purified proteins. The optimum method for reconstitution of purified Get1 or Get2 was empirically determined after testing various detergents and reconstitution methods (Supplementary Fig. 17) The precise method of reconstitution proved to be important for obtaining maximally functional proteoliposomes. The incorporation and activity of Get1 and Get2 varied with different detergents. Of those tested, DBC worked the best to achieve the maximal activity of Get1 and Get2. Every batch of DBC requires some degree of optimization with respect to the amount of Biobeads used for detergent removal. For a standard reconstitution reaction, 100 µl of reconstitution buffer (50 mM HEPES-KOH, pH 7.4, 500 mM potassium acetate, 5 mM magnesium acetate, 250 mM sucrose, 1 mM DTT, 0.25% DBC) was mixed with 10 µl of liposome (200 µg) and purified Get1 or Get2 at the desired concentration. For preparation of liposomes used as controls in the assays, purified proteins were omitted. This mixture was added to between 25 and 30 mg of Biobeads (optimized for each batch of DBC), and incubated with overhead mixing for 12 h at 4 °C. The fluid phase was separated and diluted with five volumes of ice-cold water. In some instances, the proteoliposomes were mixed with Get3 and incubated for 15 min at 25 °C, followed by 30 min at 4 °C with shaking, to allow binding. After dilution, the liposomes were sedimented in a TLA100.3 rotor in micro-test tubes at 304,290*g* for 30 min at 4 °C. The proteoliposomes were resuspended in 25 µl of membrane buffer as above. SDS–PAGE Coomassie staining and immunoblots were performed to assess the efficiency of protein incorporation; the rhodamine-PE served as a marker for lipid recovery. Typical recovery for Get1 and Get2 reconstitution was ~50%.

Multi-angle light scattering. The absolute molecular masses of individual proteins and complexes were measured by static multi-angle light scattering. Purified samples were injected onto a Superdex 200 HR 10/30 gel filtration column (GE Healthcare) equilibrated with 10 mM Tris, pH 7.5, 150 mM NaCl and 2 mM DTT. The purification system was coupled to an online, static, light-scattering detector (Dawn HELEOS II, Wyatt Technology), a refractive-index detector (Optilab rEX, Wyatt Technology) and a ultraviolet-light detector (UPC-900, GE Healthcare). Absolute weight-averaged molar masses were calculated using the ASTRA software (Wyatt Technology).

Receptor fragment binding assays. Gel-filtration-purified, 6×His-tagged Get1(21–104), Get2(1–106) and Get3 (wild type and D57N) proteins were labelled with amine-reactive succinimidyl esters of Alexa488 or Alexa594 (Invitrogen). Labelling reactions were carried out by incubating ~150 µM protein and ~600 µM dye for 1 h at room temperature (23 °C) in 100 mM $NaHCO_3$, pH 8.3, and 200 mM NaCl. After labelling, proteins were desalted and concentrated in Amicon Ultra filtration units (Millipore) to ~100 µM in 20 mM HEPES, pH 7.5, and 200 mM NaCl (receptor fragments) or 20 mM HEPES, pH 7.5, 200 mM NaCl and 2 mM DTT (Get3), and stored in aliquots at −80 °C. Protein concentration was determined using calculated A_{280} extinction coefficients after correcting for dye absorbance. Under these labelling conditions, we typically observed ~0.5–1.5 mol of dye per mole of protein.

Dissociation constants (K_d) were determined by titrating a fixed amount of labelled, nucleotide-free Get3 with labelled Get1c or Get2c. Fluorescence measurements were made in 96-well format using a Safire2 (Tecan) plate reader. Alexa594-labelled fragments were excited by fluorescence resonance energy transfer from Alexa488-labelled Get3 (wild type or D57N), using excitation and emission wavelengths of 495 and 615 nM, respectively. All experiments were carried out in 150 µl of 50 mM HEPES, pH 7.5, 100 mM NaCl, 5 mM $MgCl_2$, 5% glycerol, 0.02% Tween20 and 2 mM DTT. Blank titrations were carried out in the absence of labelled Get3 and were subtracted from the respective titration curves obtained in the presence of labelled Get3. The difference curves were evaluated by nonlinear regression using the following quadratic binding equation: $\Delta Y = 0.5B_{max}/P(K_d + P + X - \sqrt{((K_d + P + X)^2 - 4PX)})$, where B_{max} is the amplitude, P is the total concentration of labelled Get3, and X is the total concentration of labelled Get1c or Get2c.

Chase titrations were carried out by measuring fluorescence resonance energy transfer between Alexa488-labelled Get3 (wild type or D57N) and Alexa594-labelled fragments in the presence of increasing concentrations of an unlabelled fragment or nucleotide. Blank titrations were performed in the absence of labelled Get3 and were subtracted from the respective titration curves obtained in the presence of labelled Get3. The difference curves were evaluated by nonlinear regression using the following equation: $\Delta Y = F_{end} + B_{max}P/(P + K_{d,labelled}(1 + X/K_d))$, where F_{end} is the signal at saturation, B_{max} is the amplitude of the signal change, P is the total concentration of labelled fragment, $K_{d,labelled}$ is the dissociation constant of the Get3 fragment complex, X is the total concentration of the unlabelled component and K_d is the dissociation constant of the unlabelled component.

Nucleotide binding assays. Fluorescence measurements were made in 96-well format using a Safire2 plate reader with excitation and emission wavelengths of 285 and 446 nm, respectively (Supplementary Fig. 18). All experiments were carried out with gel-filtration-purified, 6×His-tagged Get3 (D57N) in 150 µl of 50 mM HEPES, pH 7.5, 100 mM NaCl, 5 mM $MgCl_2$, 5% glycerol, 0.02% Tween20 and 2 mM DTT. The dissociation constant of mant-ATP was measured by incubating 1 µM of Get3 (D57N) with increasing concentrations of mant-ATP (Molecular Probes). Dissociation constants of unlabelled nucleotides were determined by incubating 1 µM Get3 (D57N) with 1 µM mant-ATP and chasing with increasing concentrations of the corresponding unlabelled nucleotide. In each case, blank titrations were performed in the absence of Get3 and were subtracted from titration curves obtained in the presence of labelled Get3. ATP and ADP concentrations were determined by absorbance ($\varepsilon^{259} = 15{,}400\ M^{-1}\ cm^{-1}$). Dissociation constants were determined by curve fitting as described above.

Tail-anchored substrate release assay. Get3–substrate complexes were assembled by *in vitro* translation in a phenyl- and DEAE-Sepharose-depleted RRL[10] supplemented with 6×His–Get3 at ~2 µg ml^{-1}. This translation extract lacks endogenous TA binding proteins (particularly TRC40 and Bag6). Translation of the TA substrate in this system was verified to result in Get3–substrate complexes by crosslinking, and was functional as judged by Get1/2-dependent insertion (data not shown). Complexes generated by this method were mixed with the fragments or proteoliposomes as indicated in the figure legends, incubated for 30 min at 32 °C and subjected to crosslinking with disuccinimidyl suberate as described previously[8]. The samples were denatured in 1% SDS, diluted tenfold in 1% Triton X-100 buffer and subjected to pull-downs of 6×His–Get3 with immobilized Co^{2+} bound to chelating Sepharose (GE). The Get3–substrate crosslink was visualized by autoradiography.

Preparation of Get3 receptor fragment complexes for crystallization. The gene encoding native, full-length *S. cerevisiae* Get3 was subcloned into pET19b (Novagen). For co-expression with N-terminal 6×His-tagged Get1(21–104), plasmids were co-transformed into *E. coli* BL21(DE3)/pRIL (Novagen). Proteins were expressed at 37 °C for 3 h by induction with 0.1 mM IPTG after the cells reached an A_{600} of ~0.6. Cells were disrupted and purified by nickel-affinity chromatography as described above for the Get1 and Get2 fragments. Protein was eluted in buffer B containing 200 mM imidazole, and then dialysed into 10 mM Tris, pH 7.5, 100 mM NaCl, 2 mM DTT and 40% glycerol. This was followed by cleavage with 6×His-tagged TEV protease and removal of residual uncleaved Get1 fragments and the 6×His-tagged TEV protease by subtractive Ni-NTA purification. Finally, the complex was separated from excess Get1 fragments by gel filtration. Fractions were pooled, concentrated to ~10 mg ml^{-1} in 10 mM Tris, pH 7.5, 100 mM NaCl and 2 mM DTT, and stored in aliquots at −80 °C.

Co-expression of native Get3 and N-terminal 6×His-tagged Get2(1–106) or Get2(1–38) was performed as above, except that proteins were expressed at 25 °C for 6–8 h after induction. Following cell lysis and purification by nickel-affinity chromatography, the protein was dialysed into 10 mM Tris, pH 7.5, 200 mM NaCl and 2 mM DTT. This was followed by cleavage with 6×His-tagged TEV protease and subtractive Ni-NTA purification. Finally, the complex was separated from excess Get2 fragments by gel filtration. Fractions were pooled, concentrated to ~15–20 mg ml^{-1} in 10 mM Tris, pH 7.5, 150 mM NaCl and 2 mM DTT, and stored in aliquots at −80 °C.

Crystallization. Crystals of *S. cerevisiae* Get1(21–104) in complex with *S. cerevisiae* Get3 were grown at room temperature using hanging-drop vapour diffusion by mixing equal volumes of a protein solution with a reservoir solution containing 0.2 M K/Na tartrate, 16% PEG 3350, 0.1 M HEPES, pH 7.2, and 6% polypropylene

glycol P400. Crystals were cryoprotected in mother liquor supplemented with 20% ethylene glycol, and flash-frozen in liquid nitrogen.

Crystals of *S. cerevisiae* Get2(1–38) in complex with *S. cerevisiae* Get3 and ADP•AlF_4^- were grown at room temperature using hanging-drop vapour diffusion by mixing equal volumes of a protein solution containing 2 mM ADP, 2 mM $MgCl_2$, 2 mM $AlCl_3$ and 8 mM NaF with a reservoir solution containing 30% PEG 3350, 0.3 M ammonium acetate and 0.1 M Bis-Tris, pH 6.0. Crystals were briefly soaked in mother liquor supplemented with 20% ethylene glycol and flash-frozen in liquid nitrogen.

Structure determination and refinement. All data were collected at 100 K at APS beamline 21-IDG ($\lambda = 0.97856$ Å) and processed using HKL2000 (HKL Research). Data collection and refinement statistics are listed in Supplementary Table 1.

The structure of the Get1(21–104) complex with Get3 was determined to a resolution of 3.0 Å by molecular replacement with PHASER[35], using the open-dimer (nucleotide-free) form of *S. cerevisiae* Get3 (PDB ID, 3H84[20]; with the α-helical subdomain removed) as the search model. No solution could be obtained using the closed-dimer form of *S. cerevisiae* Get3 as the search model. Clear density was observed for the helical Get1 fragment and portions of the Get3 α-helical subdomain in the initial electron density maps. Model building and refinement were carried out in PHENIX[36] and COOT[37]. The final model contains one Get3 homodimer (chains A and B), two Get1 fragments (chains C and D) and one zinc atom, and was refined to an *R*-factor of 22.4% ($R_{free} = 28.2\%$). Most (94.3%) of the residues are in favoured regions of the Ramachandran plot, and 0.9% are outliers. Side-chain density is generally weakest in the α-helical subdomains, and no interpretable density was observed for residues 1–4, 97–134, 155–157, 198–219, 280–284 and 352–354 in chain A; 1–4, 99–125, 191–210, 280–284 and 352–354 in chain B; 21–35 and 103–104 in chain C; and 21–36 and 99–104 in chain D.

The structure of the Get2(1–38) complex with Get3 was determined to a resolution of 2.1 Å by molecular replacement with PHASER using a monomer of *S. cerevisiae* Get3 (PDB ID, 2WOJ[16]; with the α-helical subdomain and ligands removed) as the search model. Density for the two helices of Get2(1–38) and portions of the Get3 α-helical subdomain was clearly visible in the initial electron density maps. Model building and refinement were carried out in PHENIX and COOT. The final model contains one Get3 homodimer (chains A and B), two Get2 fragments (chains C and D), two Mg^{2+}-ADP•AlF_4^- complexes, one zinc atom and 231 water molecules, and was refined to an *R*-factor of 18.8% ($R_{free} = 23.3\%$). Again, most (98.0%) of the residues are in favoured regions of the Ramachandran plot, and 0.8% are outliers. No interpretable electron density was observed for residues 1–4, 101–126, 188–211, 280–284 and 353–354 in chain A; 1–3, 102–125, 154–158, 199–211, 280–282 and 351–354 in chain B; 1–3 and 35–38 in chain C; and 1–3 in chain D.

Miscellaneous. SDS–PAGE was done with 15% Tris-glycine or 12% Tris-tricine gels. Quantification was by phosphor imaging using a Typhoon system with accompanying software. Most images for the figures were generated by exposure to Kodak MR X-ray film. Films were digitized by scanning. Structure figures were generated with Pymol[39] and all figures were assembled using Adobe Photoshop and Illustrator.

38. Deshaies, R. J. & Schekman, R. SEC62 encodes a putative membrane protein required for protein translocation into the yeast endoplasmic reticulum. *J. Cell Biol.* **109,** 2653–2664 (1989).
39. DeLano, W. L. *PyMOL Molecular Viewer* ⟨http://www.pymol.org⟩ (2002).

doi:10.1038/nature10362

SUPPLEMENTARY FIGURES

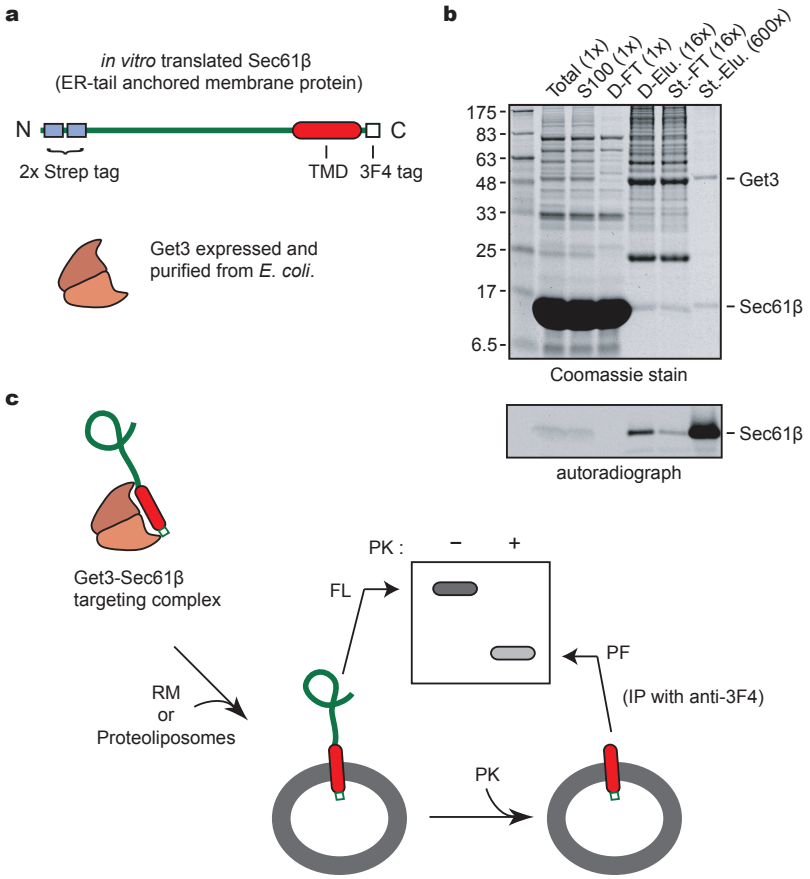

Supplementary Figure S1. Assembly, purification, and assay of a targeting complex. (a) Diagram of TA substrate used for making complexes. The N-terminal Strep tags are for targeting complex purification, while the C-terminal 3F4 tag is for the downstream insertion assay. Get3 is purified from *E. coli* as described in Mateja *et al.*, 2009, Nature, 461:361-6. (b) Purification of *in vitro* produced targeting complex. *In vitro* translation of Sec61β is performed in RRL containing ~200-fold excess (150 ng/µl) Get3. At this concentration, any endogenous TRC40 is efficiently out-competed and similar results are obtained whether translations are in total or TRC40-depleted lysates. After translation, ribosomes are removed by centrifugation and the supernatant is bound and eluted from DEAE sepharose to enrich for the complex and remove any free biotin from the translation extract. Subsequent binding and elution (with desthio-Biotin) from the StrepTactin resin results in purification of the targeting complex. Coomassie stain and autoradiograph of each step are shown. Control experiments with a mutant TA protein (containing three Arginine residues within the TMD) confirmed minimal recovery of Get3-substrate complexes subjected to the identical procedure. (c) The targeting complex is added to microsomes or proteoliposomes (typically with an ATP regenerating system), incubated (usually 30 min at 32 °C), and subjected to a PK protection assay. The products are normally immunoprecipitated with the 3F4 antibody. A schematic of the results is shown.

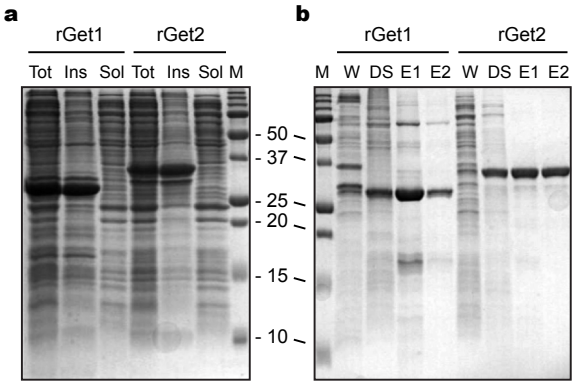

Supplementary Figure S2. Expression and purification of rGet1 and rGet2 from *E. coli*. (a) High-level expression of full-length Get1 and Get2 in *E. coli*; Tot = total lysate, Ins = crude lysate pellet, Sol = crude lysate supernatant. (b) Detergent solubilization and Ni-NTA purification of Get1 and Get2. W = impurities removed by washing the crude lysate pellet, DS = soluble fraction after detergent solubilization, E1, E2 = eluate. Note that the high molecular weight band in the purified Get1 sample is an SDS-resistant Get1 dimer as it was recognized by both anti-His and anti-Get1 antibodies on immunoblots.

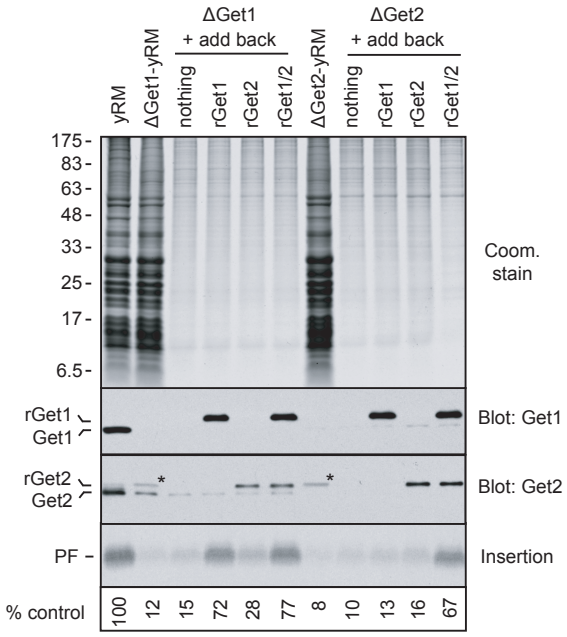

Supplementary Figure S3. Biochemical complementation of ΔGet1 or ΔGet2 microsomes. Coomassie stain, immunoblots, and insertion activity of various microsomes and proteoliposomes are shown. The 'addback' lanes are proteoliposomes prepared from either ΔGet1 or ΔGet2 yRM replenished with the indicated recombinant proteins (rGet1, rGet2, or both). Relative insertion levels are quantified. The asterisk indicates a background band in yRM (but not proteoliposomes). Note that the major coomassie staining bands observed in microsomes are either ribosomal or lumenal, and therefore not reconstituted into the proteoliposomes (which contains only integral membrane proteins).

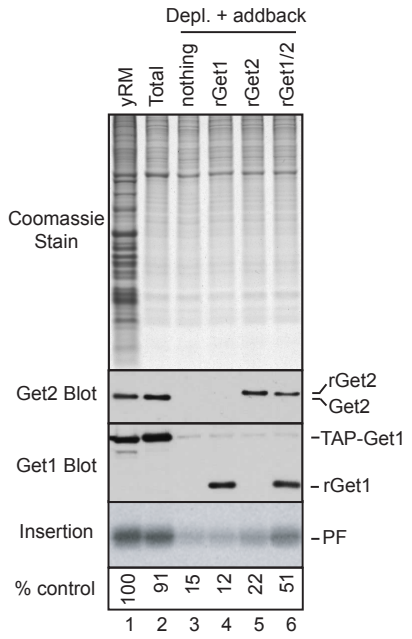

Supplementary Figure S4. Biochemical depletion and restoration of Get1/2 from yRM. Rough microsomes from a yeast strain TAP-tagged at the endogenous Get1 locus (lane 1) were solubilized and reconstituted into 'Total' proteoliposomes (lane 2). In parallel, the solubilized microsomes were depleted of Get1/2 by successive passage through an IgG-sepharose resin (to capture the TAP tag) and anti-Get1 and Get2 antibody columns (to deplete residual Get1 and Get2). The depleted lysate was either reconstituted directly (lane 3) or supplemented with recombinant Get1 and/or Get2 prior to reconstitution. Equal aliquots of the different proteoliposomes (or starting yRM) were analyzed by coomassie blue staining, immunoblotting, or insertion assays using purified Get3-Sec61β targeting complex. The numbers below the insertion gel indicate relative insertion efficiencies (with yRM set to 100%). Note that trace amounts of TAP-Get1 remain after the depletion, allowing some restoration of activity when only Get2 is added back. Also, rGet1 was reconstituted at slightly (~2-fold) lower levels than the amount in starting microsomes, leading to slightly lower restoration of activity.

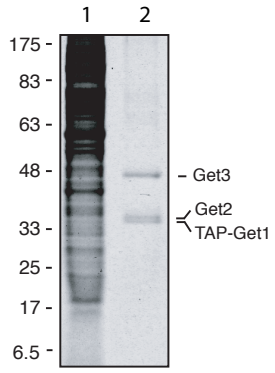

Supplementary Figure S5. Analysis of TAP-Get1 purified from yRM. Rough microsomes from a yeast strain TAP-tagged at the endogenous Get1 locus (lane 1) were solubilized and subjected to tandem affinity purification via passage through an IgG-sepharose resin, elution with TEV protease, and binding and elution from a Calmodulin affinity resin. The final purified product is shown (lane 2). The identity of Get1, Get2, and Get3 were verified by immunoblotting. Note that Get1 migrates more slowly than normal due to a portion of the TAP tag that remains on the protein. The three proteins were the only abundant proteins reliably isolated in this complex.

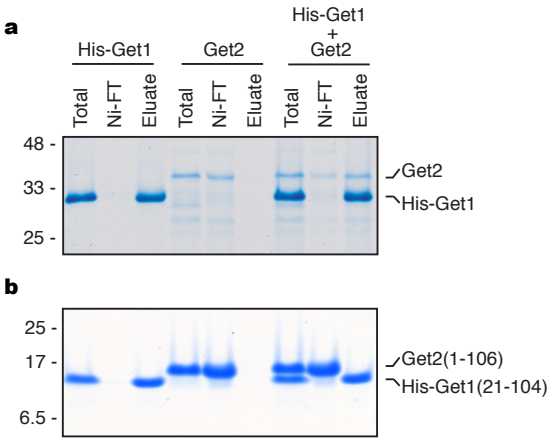

Supplementary Figure S6. Get1 and Get2 interact via their membrane domains. (a) Pulldown assay of full length Get1 and Get2. Untagged Get2 was mixed with His-Get1 in the reconstitution buffer (RB: 50mM Hepes pH 7.4, 500mM KAc, 2mM MgAc, 1mM DTT, 250mM sucrose and 0.25% Deoxy-BigCHAP).The mixture was bound to Ni-NTA agarose, washed, and eluted with imidazole. Identical pulldowns were also performed with the individual proteins. (b) Exactly as in panel a, but using the cytosolic fragments of Get1 and Get2. Note that the full length proteins interact with each other in this pulldown assay, but the cytosolic fragments do not.

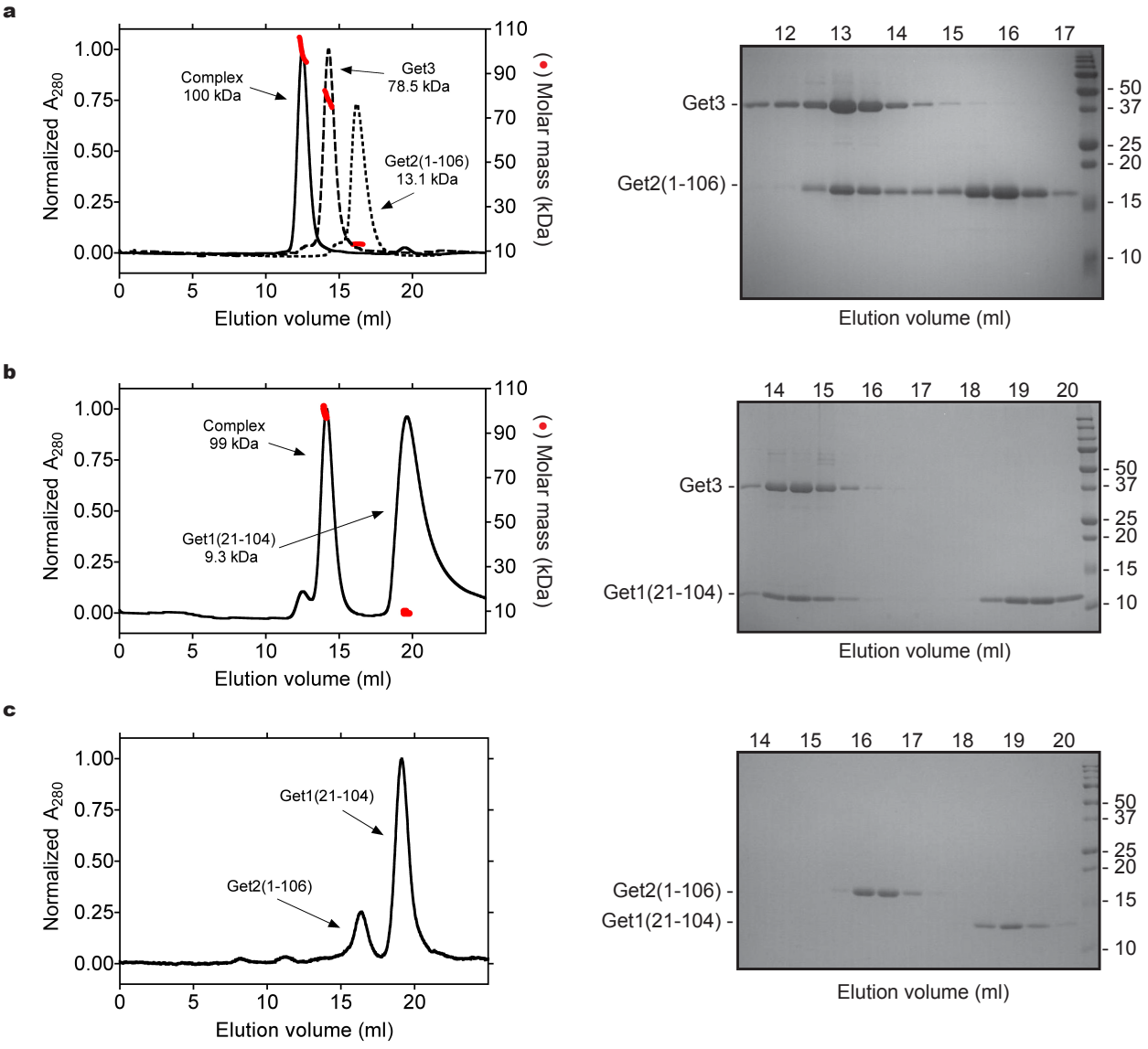

Supplementary Figure S7. Get1c and Get2c interaction analysis. (a) Get2(1-106) and (b) Get1(21-104) are, by themselves, monomeric, but associate with Get3 in a 2:2 stoichiometry. Gel-filtration elution profiles are shown (left), along with the corresponding fractions analyzed by SDS-PAGE (right). The indicated molar masses are from the MALS analysis. Note that excess fragment was added to each sample to ensure saturation. (c) SEC elution profile of an equimolar mixture of Get2(1-106) and Get1(21-104). No interaction between receptor fragments is observed.

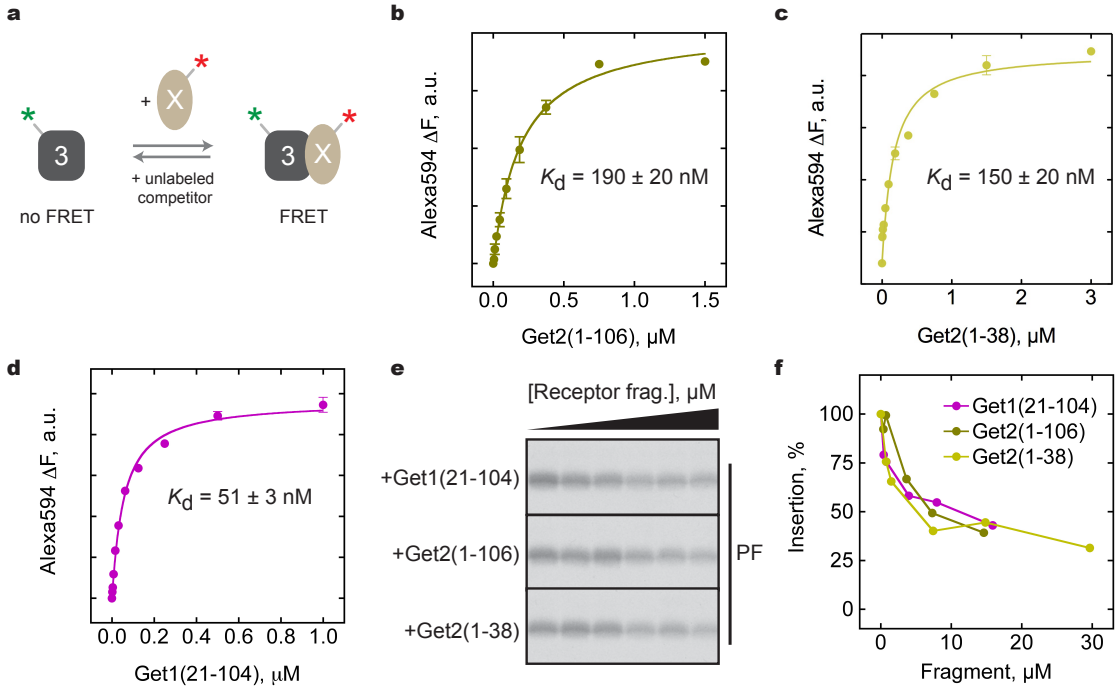

Supplementary Figure S8. The conserved, cytosolic-facing fragments of Get1 and Get2 are functional. (a) Experimental design of the FRET binding assay. Typically, Alexa488-labeled Get3 (wild-type or D57N) was incubated with a binding partner labeled with Alexa594; after excitation at 495 nm, emission is measured at 615 nm. Alternatively, fluorescence emission from preformed complex was chased by incubation with increasing concentrations of unlabeled competitor. (b-d) Fluorescence titration of nucleotide-free Get3 (10 nM) with (b) Get2(1-106), (c) Get2(1-38) or (d) Get1(21-104). (e) The fragments were also tested for the ability to inhibit TA substrate insertion into yeast-derived microsomes. The presence of protease-protected fragment (PF) was analyzed by SDS-PAGE and (f) quantified by phosphorimaging. Note that the shorter Get2(1-38) construct binds to Get3 and inhibits insertion as efficiently as the longer Get2 (1-106) construct. Measurements in (b-d) were performed in triplicate, and solid lines represent curve fits described in Methods. Error bars denote s.e.m.

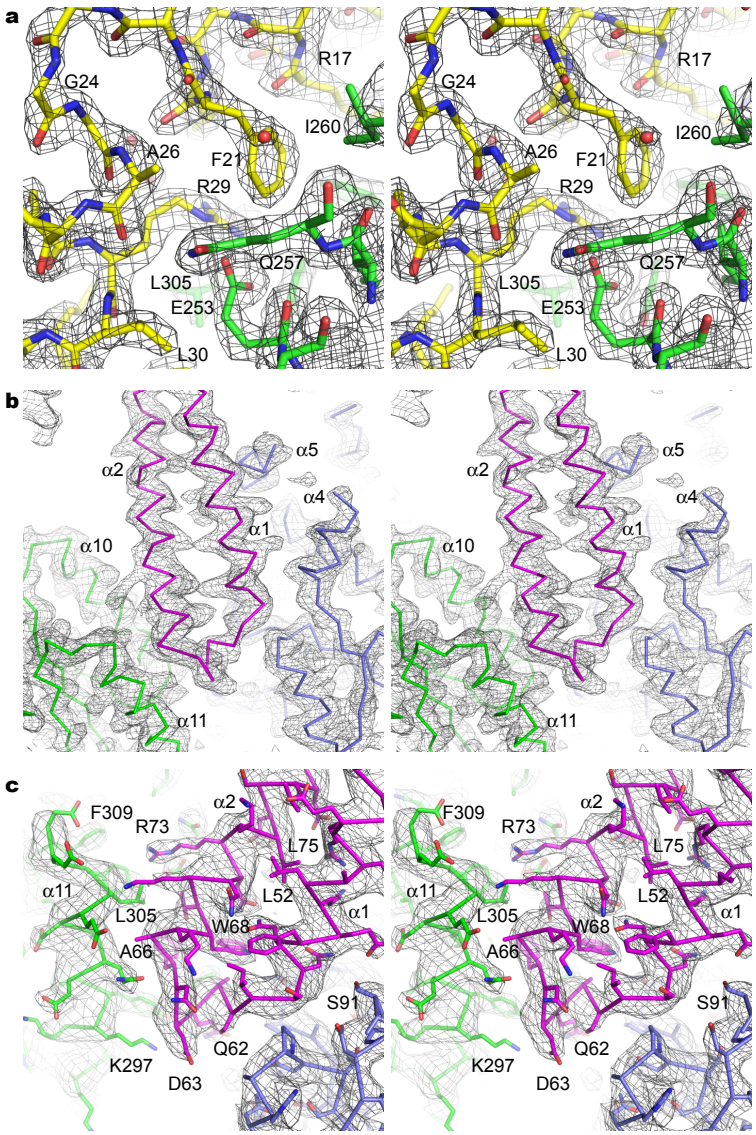

Supplementary Figure S9. Stereo views of electron density. (a) Closeup of the Get2(1-38) (yellow) interface with Get3 (green). The final refined model is superimposed onto a σ_A-weighted $2F_o$-F_c map calculated at 2.1 Å resolution, and contoured at 1.25σ. (b) Overview of the Get1(21-104) (magenta) interaction with Get3 (green and blue). The final refined model is superimposed onto a σ_A-weighted $2F_o$-F_c map calculated at 3.0 Å resolution, and contoured at 1.0σ. (c) As in b, but closeup showing sidechain interactions at the Get1(21-104) hairpin loop.

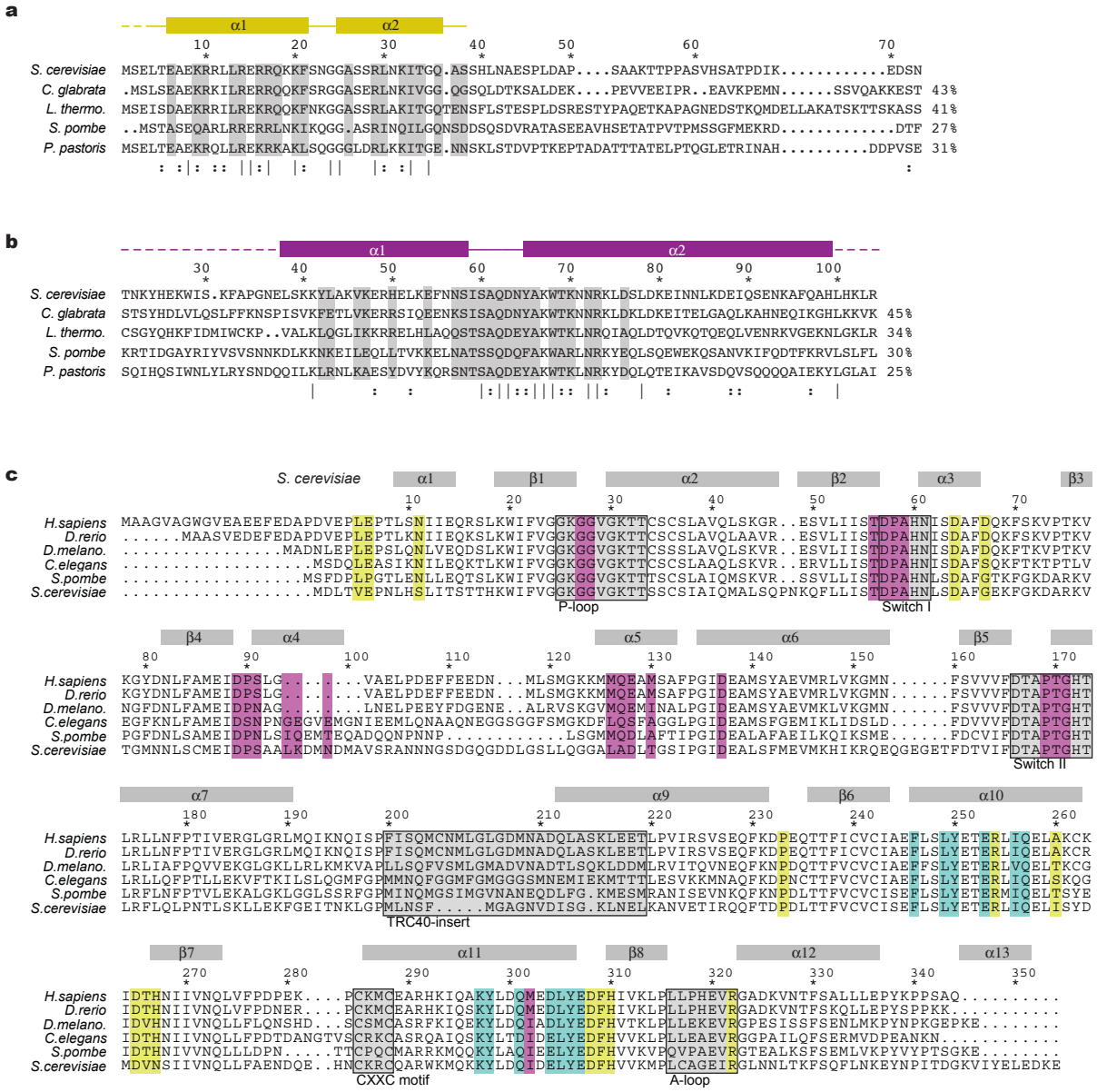

Supplementary Figure S10. Sequence alignment of (a) the N-terminal region of yeast Get2 homologs (27-43% identity to *S. cerevisiae*) and (b) the coiled-coil region of yeast Get1 homologs (25-45% identity to *S. cerevisiae*). Similar (:) and identical (|) residues are indicated. Regions that contact Get3 are shaded (grey). Secondary structural elements are shown above each alignment. (c) Sequence alignment of eukaryotic TRC40/Get3 homologs. Residues mediating interactions with Get2c (yellow), Get1c (magenta) or both (cyan) are shaded. Four conserved ATPase sequence motifs, the zinc-binding 'CXXC' motif and the 'TRC40-insert' TA substrate binding motif are shaded grey and boxed. Secondary structural elements and numbering are according to *S. cerevisiae* Get3 in the ADP•AlF_4^--bound closed dimer conformation.

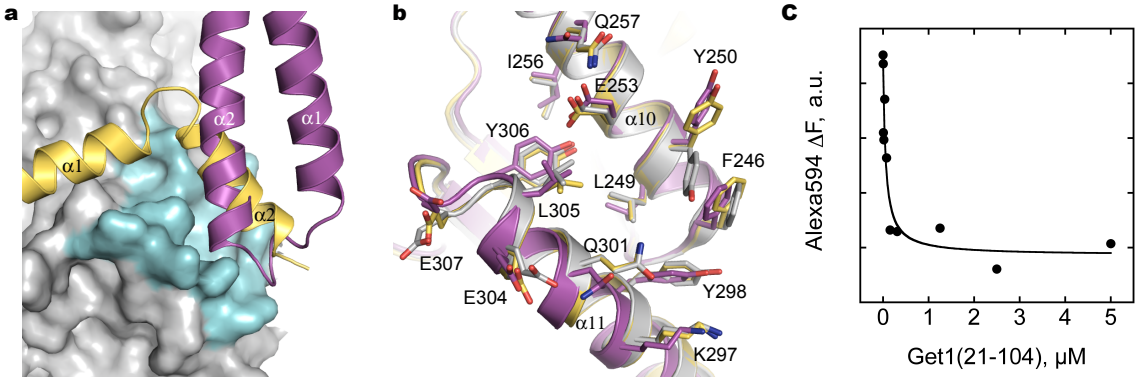

Supplementary Figure S11. The Get1 and Get2 binding sites on Get3 are partially overlapping. (a) The Get1(21-104) (magenta) open dimer complex and the Get2(1-38) (yellow) closed dimer complex were superimposed based on the structure of a single Get3 monomer. The receptor fragments bind to a partially overlapping site on the surface of Get3 (cyan). (b) This shared interface is defined by Get3 helices α10 and α11; Get3 residues that mediate interaction with Get2(1-38) (yellow) and Get1(21-104) (magenta) are indicated; one monomer from an uncomplexed, ADP•AlF_4^--bound closed dimer structure (PDB accession 2WOJ) is superimposed for reference (gray). Note the absence of any large conformational changes. (c) Nucleotide-free Get3 (10 nM) was mixed with Get2(1-106) (100 nM) and a chase titration was performed with unlabeled Get1(21-104).

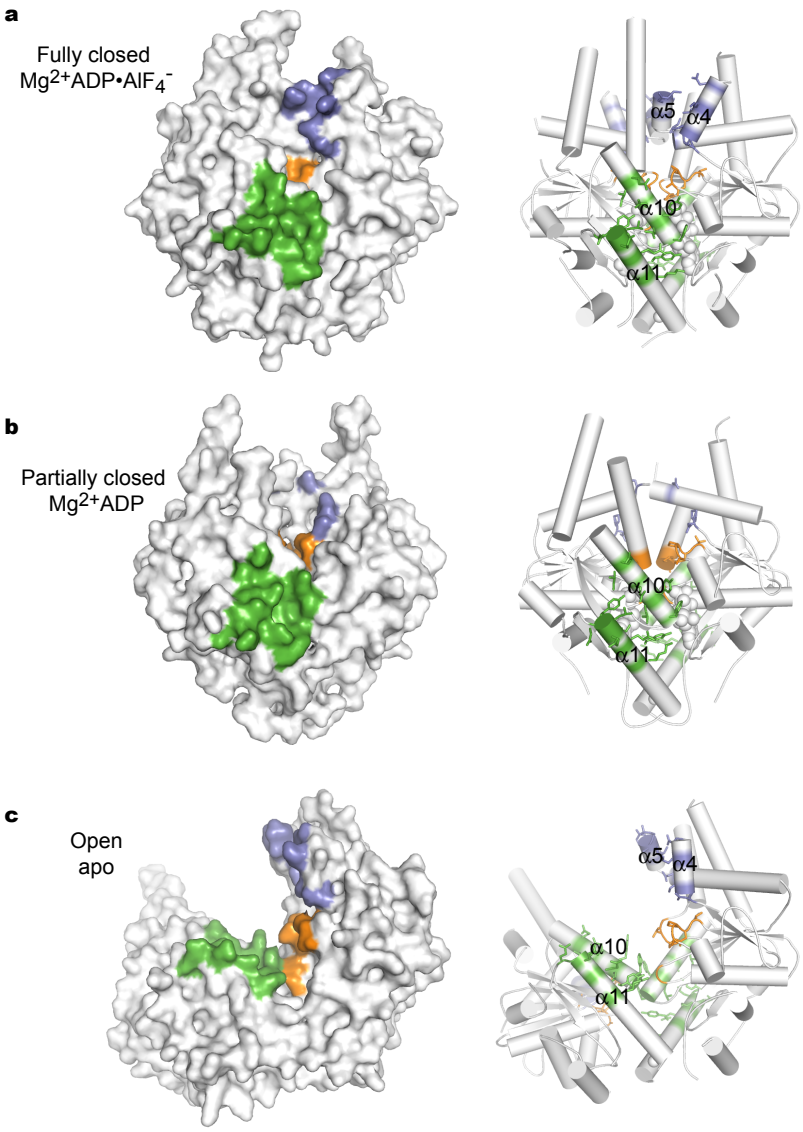

Supplementary Figure S12. Exposure of the bipartite Get1 binding site depends on the nucleotide state. Surface (left) and cartoon (right) representations of (a) the $Mg^{2+}ADP•AlF_4^-$-bound Get3 dimer. Get1 contacts to one monomer (the α10, α11-interface) are shown in green, while contacts to the second monomer are shown in blue (the α4, α5-interface) and orange (the ATPase motifs). Similar representations for (b) the $Mg^{2+}ADP$-bound Get3 dimer (PDB accession 3IQX) or (c) the nucleotide-free (apo) Get3 dimer. Note that while the entire α10, α11-interface (green) remains solvent-accessible in each conformation, the ATPase motifs (orange) and the α4, α5-interface (blue) are largely buried in the fully-closed dimer. In the $Mg^{2+}ADP$-bound partially-closed dimer, helices α4 and α5 (blue) become disordered such that the bipartite Get1 binding site is largely exposed to solvent. The structures are oriented similarly, based on structural alignment to one subunit of Get3.

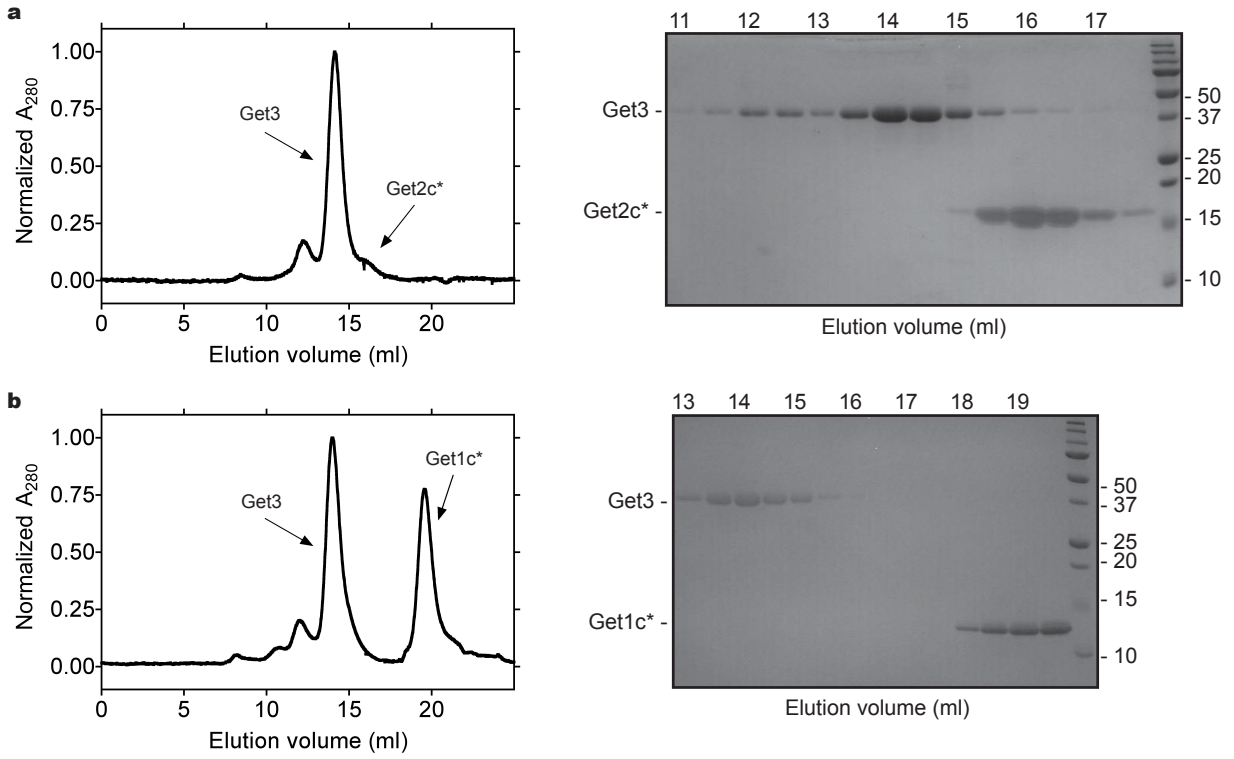

Supplementary Figure S13. Receptor fragment mutations disrupt binding to Get3. (a) Size-exclusion chromatography elution profile (left) and corresponding fractions by SDS-PAGE (right) for Get3 and the R17E mutant of Get2(1-106) (Get2c*); note the weak UV absorbance from the Get2 fragment due to its low extinction coefficient. (b) As in (a), but with Get3 and the R73E mutant of Get1(21-104) (Get1c*).

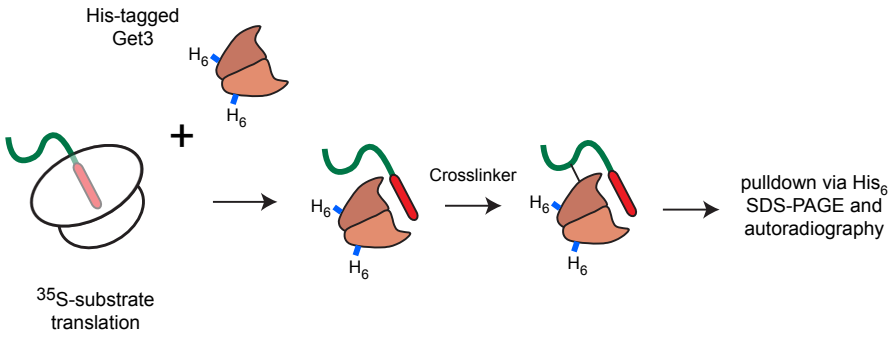

Supplementary Figure S14. Schematic diagram of substrate-Get3 crosslinking assay. Diagram of assay used to measure interactions between TA substrate and Get3. A complex between radiolabeled substrate and His-tagged Get3 is formed by *in vitro* translation (and subsequent purification in some cases). This complex is then treated as desired (e.g., incubation with Get1/2 proteoliposomes versus liposomes), then subjected to chemical crosslinking. The sample is then denatured and Get3 pulled down via the His tag. This is then analyzed by SDS-PAGE and autoradiography. Only the radiolabeled substrate is visualized, while the His pulldown ensures that only crosslinks to Get3 are captured.

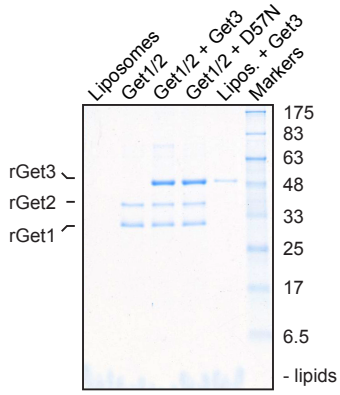

Supplementary Figure S15. Get3(D57N) interacts normally with Get1/2. Full length Get1/2 were reconstituted into proteoliposomes and after detergent removal, incubated with either wild type Get3 or Get3(D57N). The vesicles were then sedimented and analyzed by coomassie blue staining. Note that the same amount of Get3(D57N) is recovered as wild type Get3. Very little Get3 is recovered in the absence of Get1/2. Lane 1 contained no protein.

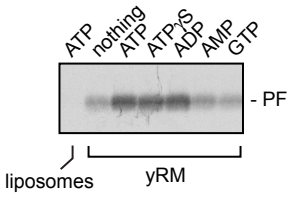

Supplementary Figure S16. Nucleotide dependence of Get3-mediated substrate insertion into yRMs. Purified Get3-Sec61β targeting complex was incubated with either liposomes or yRMs in the presence of the indicated nucleotides (each at 2 mM). After incubation, insertion was measured using the protease protection assay (as in Supplementary Figure S1). The protected fragment (PF) indicative of substrate insertion is shown.

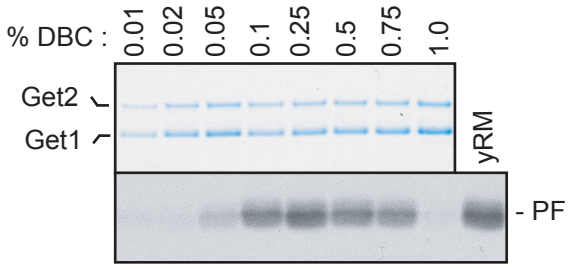

Supplementary Figure S17. Optimization of Get1/2 reconstitution. Liposomes were permeabilized/solubilized with the indicated concentration (% w/v) of DeoxyBigCHAP (DBC), mixed with a constant amount of Get1/2, and the detergent removed with Biobeads. The resulting vesicles were recovered and analyzed for protien content (upper panel) and insertion activity (bottom panel). Note that despite relatively uniform protein recovery (and lipid recovery; not shown), activity varies considerably. Such optimization was particularly important with respect to detergent concentration and Biobeads. Other detergents were also tested, with variable levels of activity. Some (e.g., CHAPS) yielded proteoliposomes with partial activity, while others (Triton X-100) were almost completely inactive. Each batch of DBC needed to be optimized as above.

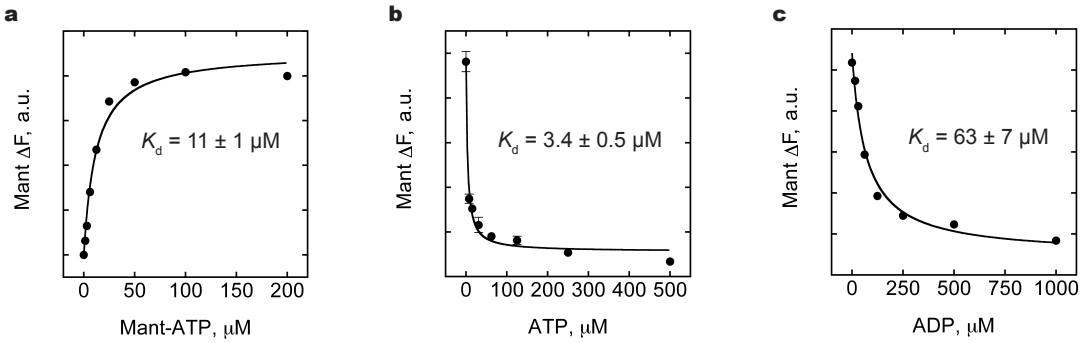

Supplementary Figure S18. ATP and ADP binding to Get3. (a) A tryptophan-to-mant FRET-based titration of an ATPase-deficient Get3 mutant (D57N) (1 μM) with mant-ATP in 50 mM HEPES, pH 7.5, 100 mM NaCl, 5 mM $MgCl_2$, 5% glycerol, 0.02% Tween 20 and 1 mM DTT. Chase titration of Get3(D57N)-mant-ATP (1 μM each) with unlabeled (b) ATP or (c) ADP. Measurements were performed in triplicate, and solid lines represent curve fits described in Methods. Error bars denote s.e.m.

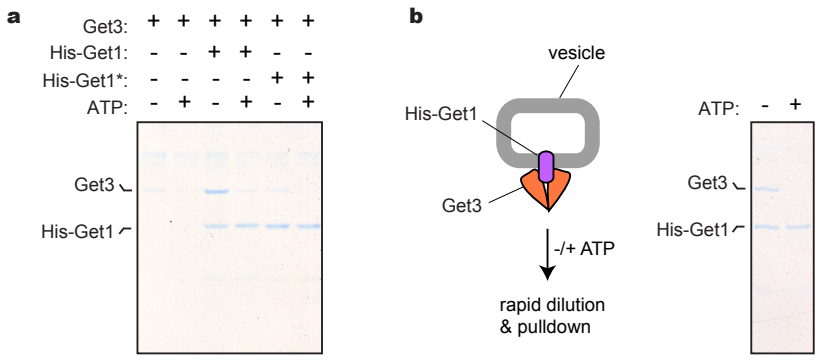

Supplementary Figure S19. The Get3 interaction with full-length Get1 is disrupted by ATP. (a) Untagged Get3 (1 µg) was mixed with 400 ng of His-Get1 or His-Get1* (the R73E mutant) in 1 ml of detergent-containing buffer (50 mM Tris, pH 7.5, 150 mM NaCl, 15 mM MgAc2, 0.5% Triton X-100, 10 mM imidazole) and subjected to pulldowns via the His-tag in the presence or absence of 5 mM ATP as indicated. Shown is the coomassie stained gel of the recovered products. Note that Get3 is efficiently pulled down with His-Get1. This interaction is largely lost in the presence of either ATP or the R73E mutation. (b) Proteoliposomes containing His-Get1 were incubated with untagged Get3 to form complexes as indicated on the left. The samples were then incubated without or with 5 mM ATP for 10 min at 25°C, after which they were rapidly diluted 10-fold into ice-cold buffer (as above) and subjected to pulldowns via the His-tag. Shown on the right is the coomassie stained gel showing that the complex is maintained in the absence of ATP, but is dissociated when ATP is included. Thus, as observed with the FRET assay using the Get1c fragment, ATP precludes an efficient interaction with Get3 in either detergent solution (panel a) or on proteoliposomes (panel b).

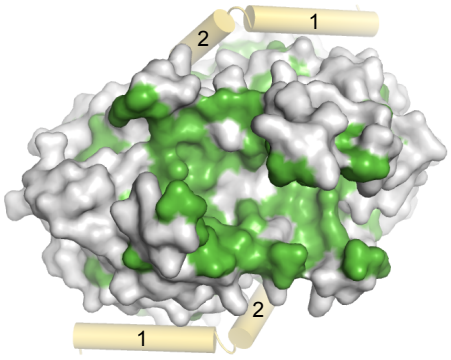

Supplementary Figure S20. The composite hydrophobic groove of ADP•AlF_4-bound Get3 remains intact in the Get2 fragment complex. A view into the hydrophobic groove of Get3, oriented as in Fig. 2b (right). Hydrophobic residues in Get3 are coloured green, and the two Get2 fragments are in yellow.

SUPPLEMENTARY TABLE

Supplementary Table 1. Data collection and refinement statistics

	Get3 + Get1(21-104)	Get3:ADP•AlF_4^- + Get2(1-38)
Data collection		
Space group	$P6_522$	$P2_12_12_1$
Cell dimensions		
a, *b*, *c* (Å)	110.3, 110.3, 316.0	52.6, 77.3, 165.8
α, β, γ (°)	90.0, 90.0,120.0	90.0, 90.0, 90.0
Resolution (Å)	50.0-3.00 (3.05-3.00)*	50.0-2.10 (2.14-2.10)
R_{sym} (%)	8.6 (72.6)	9.5 (65.9)
$I/\sigma I$	24.1 (1.7)	16.5 (1.6)
Completeness (%)	98.6 (87.3)	97.1 (89.1)
Redundancy	8.2 (4.7)	5.2 (3.9)
Refinement		
Resolution (Å)	47.2-3.0	36.5-2.1
No. Reflections	23,431	39,345
R_{cryst}/R_{free} (%)	22.4/28.2	18.8/23.3
No. atoms		
Protein	5599	5226
Ligand/ion	1	72
Water		231
B-factors (Å^2)		
Protein	111.1	36.0
Ligand/ion	112.7	21.5
Water		35.6
R.m.s. deviations		
Bond lengths (Å)	0.006	0.004
Bond angles (º)	1.0	0.83

Each dataset was obtained from a single crystal.
*Highest resolution shell is shown in parenthesis.

SUPPLEMENTARY DISCUSSION

Get3 is a targeting factor whose conformation is regulated by nucleotide (ref. 15-19). In the nucleotide free state, Get3 favors the open conformation, which is poorly suited to bind the hydrophobic TMD of TA substrates. By contrast, the ADP and ATP-bound forms of Get3 are partially and fully closed, respectively. The fully closed form appears to maximally favor substrate binding by exposing a large composite hydrophobic groove that spans both subunits of a Get3 dimer (ref. 16). Thus, it is likely to be the ATP-bound fully closed state that initially gets loaded with the TA substrate.

This conclusion fits well with the observation that ATP-bound Get3 appears to preferentially associate with Get4 (ref. 25), a subunit of the pre-targeting factor that first captures substrates after release from the ribosome (ref. 12-14). The preferential association of closed Get3 with a substrate-bound pre-targeting factor would facilitate the substrate hand-off reaction from the pre-targeting factor to Get3 (ref. 12, 13). In this manner, the targeting complex of a TA substrate bound to the closed Get3 dimer would initially contain ATP in the nucleotide binding sites.

Once a TA substrate is bound to Get3, it is very likely stabilized in the closed conformation. This is because the substrate would bridge the helical domains of the Get3 dimer, while the other end of the dimer is stabilized by a coordinated zinc ion (ref. 16). Opening of the dimer would be disfavored because of the additional energetic cost of releasing the hydrophobic substrate into the aqueous environment. Thus, nucleotide would remain trapped in the closed dimer so long as substrate remains bound. Depending when ATP hydrolysis occurs (see below), this means that the targeting complex would arrive at the membrane in an ATP- or ADP-bound, closed dimer conformation, as previously proposed (ref 17).

This view is not at odds with previous studies in which *E. coli* overexpressed recombinant Get3-substrate complexes (which are functional *in vitro*) appear to be nucleotide free (ref 6, 17). In these cases, the artificially high intracellular concentrations of substrate and Get3 may allow complex formation in the absence of ATP. Alternatively, recombinant complex formation may occur in the presence of ATP, but nucleotide (either ATP or ADP) would slowly dissociate during the multi-step, large-scale purification. Since targeting likely occurs on a rapid timescale *in vivo*, nucleotide dissociation from the targeting complex is unlikely to be physiologically relevant. Nevertheless, because these recombinant targeting complexes remain in a closed conformation, they are able to accomplish the downstream steps of targeting and substrate release *in vitro* (as described below).

At present, we do not know precisely when hydrolysis of nucleotide occurs. However, hydrolysis is obligate for substrate release at the membrane since a hydrolysis-deficient Get3 mutant (D57N) remains substrate bound and is inactive in insertion. Given that nucleotide hydrolysis must occur after substrate binding, but before substrate release, one can posit one of five possibilities: (i) substrate binding stimulates hydrolysis; (ii) Get2 binding stimulates hydrolysis; (iii) Get1 stimulates hydrolysis; (iv) lipid binding stimulates Get3 hydrolysis; (v) hydrolysis is an intrinsic property of Get3. Distinguishing between these models will require single-turnover experiments in which Get3 is first loaded with ATP, then sequentially made to interact with substrate, membrane, Get2, and Get1 while monitoring nucleotide state.

Regardless of when nucleotide hydrolysis occurs, targeting to the membrane would clearly be mediated via the closed form of Get3. The finding that the cytosolic domain of Get2 binds the closed form of Get3 without disrupting its composite hydrophobic groove strongly argues for Get2 as the initial receptor during targeting. This is attractive for several reasons. First, the region of Get2 that binds to Get3 is apparently on a long flexible tether. This may allow Get2 to act as high affinity (K_d of ~190 nM) tentacles for the targeting complex. Second, the very short region of Get2 that binds Get3 may explain why sequence homologs are very difficult to find by bioinformatics, since the remainder of Get2 would not necessarily need primary sequence conservation. Third, Get2 has a much higher affinity than Get1 for ATP-bound Get3.

In addition to these reasons in favour of Get2, several observations argue against Get1 as the initial receptor. First, the cytosolic fragment of Get1 could not be crystallized in complex with the ADP•AlF_4^- closed form of Get3. Second, the cytosolic Get1 domain is both more rigid and closer to the membrane than Get2. And third, Get1 binding to Get3 is precluded by ATP. Since ATP is probably bound to Get3 in the initial targeting complex (see above), this also makes Get1 an unlikely candidate for the initial encounter at the membrane.

Because the Get1 and Get2 binding sites on Get3 overlap, they likely interact sequentially. Given this, it seems safe to conclude that of the two proteins, Get2 makes the initial contact with the Get3-substrate targeting complex. This initial contact is apparently essential for efficient insertion since a point mutant that disrupts the Get2-Get3 interaction precludes insertion. In this situation, Get3 remains bound to its substrate, presumably unable to target to the membrane.

After binding to Get2, the targeting complex would now be close to Get1. This is because Get1 and Get2 form a tight complex with each other via their membrane domains. The implication of this is that Get1 is now present at very high local concentration. Furthermore, the rigid orientation of the Get1 coiled-coil close to the membrane contrasts with the flexible arm that tethers the Get2 N-terminal end to the membrane. Thus, in addition to the high local concentration, a potentially very strong avidity effect may allow Get1 to displace Get2 and interact with the post-hydrolysis Get3. Although this transfer reaction from Get2 to Get1 remains to be studied in greater detail, it is clear that the ability of Get1 to wedge open Get3 depends on nucleotide hydrolysis by Get3. This is conclusively illustrated by the finding that a hydrolysis mutant of Get3 (D57N) fails to release substrate upon incubation with Get1 fragment, and is inactive in insertion assays. Although non-hydrolyzable analogs of ATP were stimulatory in some earlier insertion assays (ref. 6, 17), this is not contradictory with the D57N result, as explained below.

As noted above, Get3 may arrive at Get1 with its nucleotide already hydrolyzed, or Get1 may directly stimulate hydrolysis. In either case, the result of ATP hydrolysis is to expose a portion of the bipartite Get1 binding site (α4/α5 in Get3) that is largely buried in the ATP-bound closed dimer (see Sup. Fig. S12). We posit that the partial destabilization of the closed dimer observed in the Mg^{2+}ADP-bound state (ref 17) facilitates binding of Get1. In turn, this interaction allows full opening and concomitant release of the substrate (and ADP, which binds weakly to substrate-free Get3). Consistent with this conclusion, substrate release is precluded by either the inability of Get3 to hydrolyze ATP or by a mutant Get1 that cannot interact with Get3.

The rigid orientation of the Get1 cytosolic fragment, apparently protruding perpendicular to the plane of the membrane, means that Get3 is also precisely oriented when it releases substrate. In particular, the hydrophobic groove would be parallel to and closely juxtaposed to the membrane surface. The TMD would therefore be released such that it lies on the membrane surface, an orientation that may be highly conducive to insertion. Indeed, studies with model peptide insertion into model membranes suggest that an initial parallel encounter on the membrane surface may precede and facilitate transmembrane insertion (ref. 40).

Whether TA proteins are indeed inserted in this spontaneous manner remains to be experimentally determined. The alternative view is one in which the membrane domains of Get1 and Get2 participate more actively in the insertion process itself, perhaps by 'chaperoning' the TMD into the lipid bilayer. The mechanism of actual TMD insertion in the Get pathway therefore remains an important issue for future studies.

After Get3 releases substrate, it is bound to Get1 in a nucleotide-free open dimer conformation. This interaction appears to be very stable (K_d ~50 nM, excluding avidity effects, which are likely to be substantial) and does not spontaneously dissociate in a reasonable time frame since microsomes containing Get3 can be isolated and extensively manipulated without its loss. This means that Get3 bound to Get1 would block subsequent targeting complexes from interacting, thereby hindering their ability to mediate the next round of TA protein insertion. This problem is resolved by ATP binding to Get3 in the Get1-Get3 complex. With both the Get1 fragment and with full length Get1, interaction with Get3 was disrupted by ATP. At high (millimolar) concentrations ADP also dissociates this complex, but ATP-dependent recycling would dominate under physiological conditions.

We believe this now explains the earlier findings that insertion of a recombinant pre-formed Get3-substrate complex is stimulated by free ATP (ref. 6, 17). This is because these assays used crude microsomes, in which endogenous Get3 (or its mammalian homolog TRC40) is bound to the receptor. Thus, effective insertion in such a system needs the receptor to be vacated, a reaction that occurs upon ATP binding to the membrane-bound Get1-Get3 complex. Because this dissociation does not need ATP hydrolysis, and also works with ADP to some extent, these earlier insertion assays worked with these nucleotides as well. Consistent with this interpretation, we were able to easily reproduce the earlier results with crude microsomes, but saw that the nucleotide stimulation disappeared when Get1/Get2 proteoliposomes were used instead. Likewise, removing Get3 from the crude microsome system abolished the nucleotide dependence, while pre-binding Get3 to the Get1/2 proteoliposomes restored ATP-dependence. Thus, ATP binding to Get3 both releases it from Get1 and prepares it for being loaded with the next TA protein substrate.

SUPPLEMENTARY NOTES

Figure 1

Panel a – Successful insertion of the TA protein is assayed by the production of a protease-protected fragment (PF) representing the inserted TMD (see Sup. Fig. S1). Get1 and Get2 levels are reduced in the ΔGet2 and ΔGet1 strains, respectively. The recovery of Get3 in these microsome preps is not due to specific membrane binding. Rather, in the absence of Get2 or Get1, Get3 forms aggregates (ref. 7), which co-sediment with the crude microsomes. Indeed, we have confirmed that Get3 is readily salt-extracted from ΔGet1 and ΔGet2 yRMs, but not wild type yRMs (unpublished observations). Thus, the co-sedimentation of Get3 with microsomes deleted of its receptor proteins should not be interpreted as evidence for an alternate receptor.

Panel b – The recombinant proteins migrate slightly slower due to His-tags.

Panel d – The constructs are all identical, but with different TMDs from the indicated proteins. The N-terminal domain is a double-Strep II tagged version of Sec61β.

SUPPLEMENTARY REFERENCES

40. Reshetnyak, Y.K., Andreev, O.A., Segala, M., Markin, V.S. & Engelman, D.M. Energetics of peptide (pHLIP) binding to and folding across a lipid bilayer membrane. *Proc Natl Acad Sci USA* **105**, 15340-15345 (2008).